ELECTRICAL IMPEDANCE SPECTROSCOPY AND TOMOGRAPHY: APPLICATIONS ON PLANT CHARACTERIZATION

A Thesis Submitted to the College of Graduate and Postdoctoral Studies

In Partial Fulfillment of the Requirements

For the Degree of Master of Science

In the Department of Electrical and Computer Engineering

University of Saskatchewan

Saskatoon SK, Canada

By

MONZURUL ISLAM

PERMISSION TO USE

In presenting this thesis in partial fulfillment of the requirements for a Postgraduate degree from the University of Saskatchewan, I agree that the Libraries of this University may make it freely available for inspection. I further agree that permission for copying of this thesis in any manner, in whole or in part, for scholarly purposes may be granted by the professor or professors who supervised my thesis/dissertation work or, in their absence, by the Head of the Department or the Dean of the College in which my thesis work was done. It is understood that any copying or publication or use of this thesis or parts thereof for financial gain shall not be allowed without my written permission. It is also understood that due recognition shall be given to me and to the University of Saskatchewan in any scholarly use which may be made of any material in my thesis.

Requests for permission to copy or to make other uses of materials in this thesis in whole or part should be addressed to:

Head of the Department of Electrical and Computer Engineering
57 Campus Drive
University of Saskatchewan
Saskatoon, Saskatchewan
Canada, S7N 5A9
OR
Dean
College of Graduate and Postdoctoral Studies
University of Saskatchewan
116 Thorvaldson Building, 110 Science Place
Saskatoon, Saskatchewan, S7N 5C9
Canada.

ABSTRACT

World population will grow to 9.6 billion by 2050 and global food production needs to be increased by 70% to feed the increased population. Hence, better insight into plant physiology can impart better quality in fruits, vegetables, and crops, and eventually contribute to food security and sustainability. In this direction, this thesis utilizes electrical sensing technology, electrical impedance spectroscopy (EIS) and tomography (EIT), for better understanding and characterization of a number of physiological and structural aspects of the plant. It investigates the dehydration process in onion and ripening process in avocado by EIS, and perform 3D structural imaging of root by EIT.

The thesis tracks and analyzes the dynamics of natural dehydration in onion and also assesses its moisture content using EIS. The work develops an equivalent electrical circuit that simulates the response of the onion undergoing natural drying for a duration of three weeks. The developed electrical model shows better congruence with the experimental data when compared to other conventional models for plant tissue with a mean absolute error of 0.42% and root mean squared error of 0.55%. Moreover, the study attempts to find a correlation between the measured impedance data and the actual moisture content of the onions under test (measured by weighing) and develops a simple mathematical model. This model provides an alternative tool for assessing the moisture content of onion nondestructively. The model shows excellent correlation with the ground truth data with a deterministic coefficient of 0.977, root mean square error of 0.030 and sum of squared error of 0.013.

Next, the thesis presents an approach that will integrate EIS and machine learning technique that allows us to monitor ripening degree of avocado. It is evident from this study that the impedance absolute magnitude of avocado gradually decreases as the ripening stages (firm, breaking, ripe and overripe) proceed at a particular frequency. In addition, Principal component analysis shows that impedance magnitude (two principal components combined explain 99.95% variation) has better discrimination capabilities for ripening degrees compared to impedance phase angle, impedance real part, and impedance imaginary part. The developed classifier utilizes two principal component features over 100 EIS responses and demonstrate classification over firm,

breaking, ripe and overripe stages with an accuracy of 90%, precision of 93%, recall of 90%, f1-score of 90% and an area under ROC curve (AUC) of 88%.

Later on, this thesis presents the design, development, and implementation of a low-cost EIT system and analyzes root imaging as well. The designed prototype consists of an electrode array system, an Impedance analyzer board, 2 multiplexer units, and an Arduino. The Eval-Ad5933-EBZ is used for measuring the bio-impedance of the root, and two CD74HC4067 Multiplexers are used as electrode switching unit. Measuring and data collecting are controlled by the Arduino, and data storage is performed in a PC. By performing Finite Element Analysis and solving forward and inverse problem, the tomographic image of the root is reconstructed. The system is able to localize and build 2D and 3D tomographic image of root in a liquid medium. This proposed low-cost and easy-to-access system enables the users to capture the repetitive, noninvasive and non-destructive image of a plant root. Furthermore, the study proposes a simple mathematical model, based on ridge regression, which can predict root biomass from EIT data nondestructively with an accuracy of more than 93%. Thus, this study offers plant scientists and crop consultants the ability to better understand plant physiology nondestructively and noninvasively.

ACKNOWLEDGEMENTS

I would like to express my deep and sincere gratitude to my supervisors, Professor Khan A. Wahid and Anh Dinh, for supervising my work. I owe to both of them for their constant supervision, encouragement, personal guidance during the progress of my thesis. Starting with a little background in Electrical Sensing, I was able to acquire content knowledge and contribute to the advancement of the state-of-the-art research with their valuable guidance and continual encouragement. I am privileged to have the opportunity to work under their supervision, which immensely enriched my graduate experience.

I would also like to thanks all the members of Multimedia Processing and Prototyping laboratory at the University of Saskatchewan. Finally, I would like to express my deepest gratitude and love to my family and friends for their unconditional love, care, and support at each step of my life.

TABLE OF CONTENTS

LIST OF TABLES

LIST OF FIGURES

ABBREVIATIONS AND SYMBOLS

AC	Alternating Current
AUC	Area Under Curve
CPE	Constant Phase Element
EIS	Electrical Impedance Spectroscopy
EIT	Electrical Impedance Tomography
EPI	Electrode Polarization Interference
FEM	Finite Element Method
GN	Gauss Newton
Hz	Hertz
MRI	Magnetic Resonance Imaging
PCA	Principal Component Analysis
ROC	Receiver Operating Curve
SUT	Sample Under Test
SVM	Support Vector Machine
TPR	True Positive Rate
TNR	True Negative Rate
C	Capacitance
L	Inductance
R	Resistivity
X	Imaginary part of impedance
Z	Complex impedance
σ	Conductivity
θ	Phase angle

Chapter 1 – Introduction

1.1 Introduction

World population will grow to 9.6 billion by 2050, and global food production needs to be increased by 70% to feed the increased population [1]. Hence, analyzing and understanding plant tissue can contribute towards the superior quality of vegetables and fruits. Gaining an insight into plant's health and root system can impart better crop performance and eventually contribute to food security and sustainability. Therefore, plant tissue characterization is one of the major thrust of today's engineering research. Numerous efforts have been made to devise an accurate and easily accessible technique for investigating plant physiology. Conventional chemical and biochemical analyses conducted to investigate plant physiology are limited by factors like processing time and destructive nature [2]. These methods are often laborious, expensive and require access to the laboratory facility. Moreover, these methods are infeasible for a repetitive inspection. Nondestructive methods like Magnetic Resonance Imaging (MRI) and CT Scan are found to be effective towards the understanding of fruits' and vegetables' quality and postharvest processing [3, 4]. Both MRI and CT are limited by factors such as high cost and processing complexity. Hyperspectral imaging can effectively assess various characteristics of plants [5] but it also suffers from constraints like cost and processing. Therefore, it is essential to expand the technologies from different viewpoints.

Developing a relationship between food qualities and engineering properties of food is the main challenge of today's food engineering. The electrical properties of food are found to be closely related to food quality. Moreover, electrical sensing is found to uncover the fundamental attributes in plants and to follow physiological progressions due to environmental impacts [6]**.** Electrical Impedance Spectroscopy (EIS) is one of the methods of measuring electrical characteristics with a small amplitude sine wave voltage (or current) [7]. Impedance spectrum can be determined using a multi-frequency impedance analyzer by observing the electrical response of tissues to the passage of the external power [7]. EIS can allow insight into the physiological and pathological information on biological tissues and organs. Electrical Impedance Tomography is another electrical sensing technology where electrical conductivity, permittivity, and impedance of an object is measured by an array of electrodes around it and by utilizing the measured data at

domain boundary, a tomographic image of the object is reconstructed [8-10]. Both EIS [7] and EIT [11, 12] modules are fast, low-cost, radiation-free, nondestructive and noninvasive.

EIS has demonstrated valuable impact on food quality and stability monitoring over the last decades. It is found to offer a great insight into the physiology of fruits and vegetables undergoing the natural drying process. Apples properties during 21 days of aging were monitored using EIS to provide information about the physical properties of apple [13]. Two different analytical techniques for assessment of the changes of apples' properties during the aging time were proposed. The first one is a single measurement in the low frequency range (around 100Hz) and the second one is a multi-frequency argand plot on a complex plane. The results propose that alteration in observed EIS can be attributed to the changes in the relative moisture content of the apple. Kertész, et al. [14] utilized EIS to measure the electrical response of carrot slice during drying by HP 4284A and 4285A precision LCR meters in the frequency range from 30Hz to 1MHz and from 75kHz to 30MHz, respectively, at a voltage of 1V. By measuring the weight of the samples with a with a DenverSI-603 electronic analytical and precision balance, the moisture content was calculated on a wet basis. Moisture content was found to decrease according to a polynomial function and alteration of impedance during drying showed good correlation with change in moisture content. Ando, et al. [15] investigated EIS to explore the changes in the cell physiological status of potato tissues during hot air drying at 50–80^{0}C. At the early drying stage, from the initial moisture content to moisture content of 1.0 (dry basis), the modified Hayden model was found to be useful to describe the impedance characteristics. Considering the benefits of EIS as an easily accessible and nondestructive tool, this work proposes to use it to understand the mechanisms of dehydration on onion and to assess its moisture content.

EIS technique is found to offer insight into the physiology of fruits undergoing the ripening process. In order to assess the freshness of banana, EIS investigation was performed during different ripening state [16]**.** By attaching Ag/AgCl electrode and injecting a small amount of current, impedance responses are measured by the 4294A Impedance Analyzer over a frequency range of 50Hz to 1MHz. The impedance magnitude, phase angle, real and imaginary part varied markedly with the alteration of ripening state. Authors [17] designed a nondestructive device to obtain the impedance spectrum of the whole strawberry fruit and later on performed classification by utilizing corresponding equivalent circuit parameters (Constant Phase Element, CPE-P, and $R_{infinity}$). The study showed that the strawberries at the highest stage of ripeness had significantly

lower constant phase element and Ro (extra-cellular resistance) values compared to other strawberries. Neto, et al. [18] utilized the EIS technique for the determination of the maturation degree of mangoes based on the variation of bulk resistance dependence with the maturation of fruits. The authors in the article came up with this strategy to normalize bulk resistance by diameter to compensate the size variations of samples. The work demonstrated good agreement between the variation of electrical response and mechanical response of fruit. Montoya, et al. [19] investigated that electrical conductivity could be a suitable factor for assessment of quality during ripening and cold storage. The found some resemblance between electrical conductivity response and ethylene productions curve. They defined a threshold of conductivity (0.24 S/m) that indicates the limiting value for fruit stored at non-injurious temperatures and subsequently transferred to 20°C for marketing. Chowdhury, et al. [20] carried out EIS study on mandarin orange fruit during ripening in a spectrum between 50Hz to 1MHz. They observed significant variation of the impedance, phase angle, real and imaginary part of the impedance with the different state of orange ripening. The study also demonstrated the loss of weight of corresponding samples with the progression of ripening states. This study exploits EIS to understand mechanisms of ripening on avocado and to assess its ripening degree.

EIT is a fast, low cost, noninvasive, non-ionizing, radiation-free and portable imaging modality. Due to its unique advantages, EIT has obtained enormous attention and interest in diversified fields such as medical imaging, material engineering, Nanotechnology and MEMS, civil engineering, chemical engineering, biotechnology, and other fields of engineering, technology, and applied sciences [11, 12]. In medical imaging, EIT has been extensively used for imaging of lung [21, 22], studying the regional ventilation distribution in neonatal and pediatric lung disease [23], imaging of breast [24] and brain [12]. EIT has been utilized in material engineering and the manufacturing technology such as studying the semiconductor manufacturing and estimating conductivity distribution of polysilicon thin film [25]. In nanotechnology, EIT has been studied for imaging of Carbon Nanotube (CNT) composite thin films [26, 27]. In several civil engineering applications, and a number of research works on EIT have been reported such as imaging leaks from buried pipes [28], brick walls imaging [29]. In biotechnology, EIT has been studied by several research groups for Cell culture imaging by such as [30, 31].

Although not much works are found in the literature on the application of EIT on plant root, Weigand and Kemna [32] conducted a study on structural and functional imaging of crop

root by EIT. They designed and conducted a controlled experiment in which the root systems of oilseed plants were monitored in a 2-D, water-filled rhizotron container with an array of 38 electrodes. The EIT imaging revealed low-frequency polarization response which attributed to crop root since the polarization response of water medium is insignificant. Based on a pixel-based Debye decomposition analysis of the spectral imaging results, the work found a mean relaxation time of the root system's polarization signature in a frequency of 15Hz. For functional imaging, Weigand and Kemna applied nutrition stress over 3-day period and observed a gradual decrease of polarization response from the root system. Thus they investigated the capability of EIT for imaging of root physiological process (stress). This study proposes the design and development of a low-cost EIT system from readily available off-the-shelf equipment and test the validity of the system for imaging of plant root in hydroponics.

1.2 Objective of the Thesis

The research objective of this work was to investigate and analyze the physiological, functional and structural aspects of plant by utilizing EIS and EIT method. To achieve this objective, the following endeavors were pursued:

- Investigating the prospect electrical impedance spectroscopy for nondestructive monitoring of the physiological status of onion undergoing dehydration. Then utilizing the equivalent circuit model of EIS for tracking the dehydration process.
- Exploring the feasibility of electrical impedance spectroscopy technique as an alternative tool for estimation of moisture content on the onion.
- Exploring the feasibility of electrical impedance spectroscopy for nondestructive and noninvasive monitoring of ripening process of avocado. Then assessing the ripening degrees of avocado by EIS and machine learning approach.
- Developing a low-cost, low power, portable, lightweight and automated electrical impedance tomography data acquisition system (including hardware and software) from the commercial off-the-shelf components.
- Investigating the feasibility of utilizing the EIT technique to detect plant root in hydroponics and reconstruct the 3D images.
- Exploring the prospect of EIT system to assess root biomass nondestructively.

1.3 Organization of the Thesis

A brief overview of the organization of the rest of the thesis is presented in this section. In Chapter 2, background study on the theory of EIS and EIT is presented. A case study on the application of EIS on onion is presented in Chapter 3. The feasibility of EIS on modeling the dehydration process of onion during storage is explored. Additionally, a mathematical model for nondestructive assessment of onion moisture content is presented. In Chapter 4, a study on the application of EIS and machine learning for assessment of ripening degree on avocado is presented. In Chapter 5, the design and development of a low-cost EIT system is presented and its application for root imaging is explored. Utilization of the system for nondestructive assessment of biomass is also investigated. Finally, conclusion and direction for future research are given in Chapter 6.

References

[1] T. Searchinger, C. Hanson, J. Ranganathan, B. Lipinski, R. Waite, R. Winterbottom*, et al.*, "Creating a sustainable food future. A menu of solutions to sustainably feed more than 9 billion people by 2050. World resources report 2013-14: interim findings," 2014.

[2] K. Miloski, K. Wallace, A. Fenger, E. Schneider, and K. Bendinskas, "Comparison of biochemical and chemical digestion and detection methods for carbohydrates," *American Journal of Undergraduate Research,* vol. 7, pp. 48-52, 2008.

[3] M. K. Abera, S. W. Fanta, P. Verboven, Q. T. Ho, J. Carmeliet, and B. M. Nicolai, "Virtual fruit tissue generation based on cell growth modelling," *Food and Bioprocess Technology,* vol. 6, pp. 859-869, 2013.

[4] L. Zhang and M. J. McCarthy, "Measurement and evaluation of tomato maturity using magnetic resonance imaging," *Postharvest Biology and Technology,* vol. 67, pp. 37-43, 2012.

[5] R. Khodabakhshian and B. Emadi, "Application of Vis/SNIR hyperspectral imaging in ripeness classification of pear," *International Journal of Food Properties,* vol. 20, pp. S3149-S3163, 2017.

[6] D. El Khaled, N. Castellano, J. Gazquez, R. G. Salvador, and F. Manzano-Agugliaro, "Cleaner quality control system using bioimpedance methods: a review for fruits and vegetables," *Journal of Cleaner Production,* vol. 140, pp. 1749-1762, 2017.

[7] T. K. Bera, "Bioelectrical impedance methods for noninvasive health monitoring: a review," *Journal of medical engineering,* vol. 2014, pp. 1-28, 2014.

[8] R. H. Bayford, "Bioimpedance tomography (electrical impedance tomography)," *Annu. Rev. Biomed. Eng.,* vol. 8, pp. 63-91, 2006.

[9] M. Cheney, D. Isaacson, and J. C. Newell, "Electrical impedance tomography," *SIAM review,* vol. 41, pp. 85-101, 1999.

[10] J. G. Webster, *Electrical impedance tomography*: Taylor & Francis Group, 1990.

[11] C. W. L. Denyer, "Electronics for real-time and three-dimensional electrical impedance tomographs," Oxford Brookes University, 1996.

[12] D. Holder, A. Rao, and Y. Hanquan, "Imaging of physiologically evoked responses by electrical impedance tomography with cortical electrodes in the anaesthetized rabbit," *Physiological measurement,* vol. 17, p. A179, 1996.

[13] T. Yovcheva, E. Vozáry, I. Bodurov, A. Viraneva, M. Marudova, and G. Exner, "Investigation of apples aging by electric impedance spectroscopy," *Bulg. Chem. Commun,* vol. 45, pp. 68-72, 2013.

[14] Á. Kertész, Z. Hlaváčová, E. Vozáry, and L. Staroňová, "Relationship between moisture content and electrical impedance of carrot slices during drying," *International Agrophysics,* vol. 29, pp. 61-66, 2015.

[15] Y. Ando, K. Mizutani, and N. Wakatsuki, "Electrical impedance analysis of potato tissues during drying," *Journal of Food Engineering,* vol. 121, pp. 24-31, 2014.

[16] A. Chowdhury, T. Bera, D. Ghoshal, and B. Chakraborty, "Studying the electrical impedance variations in banana ripening using electrical impedance spectroscopy (EIS)," in *Computer, Communication, Control and Information Technology (C3IT), 2015 Third International Conference on*, 2015, pp. 1-4.

[17] J. R. González-Araiza, M. C. Ortiz-Sánchez, F. M. Vargas-Luna, and J. M. Cabrera-Sixto, "Application of electrical bio-impedance for the evaluation of strawberry ripeness," *International Journal of Food Properties,* vol. 20, pp. 1044-1050, 2017.

[18] A. F. Neto, N. C. Olivier, E. R. Cordeiro, and H. P. de Oliveira, "Determination of mango ripening degree by electrical impedance spectroscopy," *Computers and Electronics in Agriculture,* vol. 143, pp. 222-226, 2017.

[19] M. Montoya, J. De La Plaza, and V. López-Rodriguez, "Electrical conductivity of avocado fruits during cold storage and ripening," *LWT-Food Science and Technology,* vol. 27, pp. 34-38, 1994.

[20] A. Chowdhury, P. Singh, T. K. Bera, D. Ghoshal, and B. Chakraborty, "Electrical impedance spectroscopic study of mandarin orange during ripening," *Journal of Food Measurement and Characterization,* vol. 11, pp. 1654-1664, 2017.

[21] N. Harris, A. Suggett, D. Barber, and B. Brown, "Applications of applied potential tomography (APT) in respiratory medicine," *Clinical Physics and Physiological Measurement,* vol. 8, p. 155, 1987.

[22] T. Meier, H. Luepschen, J. Karsten, T. Leibecke, M. Großherr, H. Gehring*, et al.*, "Assessment of regional lung recruitment and derecruitment during a PEEP trial based on electrical impedance tomography," *Intensive care medicine,* vol. 34, pp. 543-550, 2008.

[23] T. Pham, M. Yuill, C. Dakin, and A. Schibler, "Regional ventilation distribution in the first 6 months of life," *European Respiratory Journal,* vol. 37, pp. 919-924, 2011.

[24] N. M. Zain and K. K. Chelliah, "Breast imaging using electrical impedance tomography: correlation of quantitative assessment with visual interpretation," *Asian Pacific Journal of Cancer Prevention,* vol. 15, pp. 1327-1331, 2014.

[25] M. Kruger, "Tomography as a metrology technique for semiconductor manufacturing," Electronics Research Laboratory, College of Engineering, University of California, 2003.

[26] T.-C. Hou, K. J. Loh, and J. P. Lynch, "Electrical impedance tomography of carbon nanotube composite materials," in *Sensors and Smart Structures Technologies for Civil, Mechanical, and Aerospace Systems 2007*, 2007, p. 652926.

[27] T.-C. Hou, K. J. Loh, and J. P. Lynch, "Spatial conductivity mapping of carbon nanotube composite thin films by electrical impedance tomography for sensing applications," *Nanotechnology,* vol. 18, p. 315501, 2007.

[28] J. Jordana, M. Gasulla, and R. Pallàs-Areny, "Electrical resistance tomography to detect leaks from buried pipes," *Measurement Science and Technology,* vol. 12, p. 1061, 2001.

[29] J. Hola, Z. Matkowski, K. Schabowicz, J. Sikora, and S. Wójtowicz, "New method of investigation of rising damp in brick walls by means of impedance tomography," in *17th World Conference on Nondestructive Testing*, pp. 25-28, 2008.

[30] P. Linderholm, L. Marescot, M. H. Loke, and P. Renaud, "Cell culture imaging using microimpedance tomography," *IEEE Transactions on Biomedical Engineering,* vol. 55, pp. 138-146, 2008.
[31] T. Sun, S. Tsuda, K.-P. Zauner, and H. Morgan, "On-chip electrical impedance tomography for imaging biological cells," *Biosensors and Bioelectronics,* vol. 25, pp. 1109-1115, 2010.
[32] M. Weigand and A. Kemna, "Multi-frequency electrical impedance tomography as a non-invasive tool to characterize and monitor crop root systems," *Biogeosciences,* vol. 14, pp. 921-939, 2017.

Chapter 2 – Background

2.1 Theory of Bioimpedance and Electrical Impedance Spectroscopy

The plant body is a complex biological structure composed of tissues which are developed with cells suspended in extracellular fluids (ECF) [1]. Cells are composed of intracellular fluids (ICF), cell membrane (CM) and cell wall (CW). ECF, ICF and CM are developed with different materials and so exhibit distinguishable electrical attributes. The ECF and ICF act as electrolytes and provide a conducting path to applied alternating current [2]. The CM is a protein-lipid-protein (P-L-P) structure and exhibits capacitance to the current. Consequently, the overall response of the biological tissues to an alternating electrical signal generates a complex bioelectrical impedance. Mathematically, the impedance $Z\angle(\theta)$ is calculated by dividing the voltage ($V\angle(\theta_1)$) measured by applied current ($I\angle(\theta_2)$) as shown in equation (2.1)

$$Z\angle(\theta) = \frac{V\angle(\theta_1)}{I\angle(\theta_2)} \tag{2.1}$$

Bioimpedance is a complex quantity which varies with tissue composition and frequency of the applied signal. Therefore, the frequency dependent bioimpedance can be represented as shown in equation (2.2)

$$\mathrm{Z}_b(\omega) = \mathrm{Re}(Z(\omega)) - j\,\mathrm{Im}(Z(\omega)) = R_b(\omega) - jX_b(\omega) \tag{2.2}$$

where, $\mathrm{Re}(Z(\omega)) = R_b(\omega)$ and $\mathrm{Im}(Z(\omega)) = X_b(\omega)$ represent the magnitude of the real part of the complex $\mathrm{Z}_b(\omega)$ and the magnitude of the imaginary part of the complex $\mathrm{Z}_b(\omega)$, respectively.

Bioimpedance is sensitive to the physiological status of plant tissue. Again, as the response of bioimpedance changes with frequency, a multi-frequency impedance analysis can offer better insight into plant physiology and better understanding to plant tissue status. Electrical impedance spectroscopy (EIS) is a multi-frequency analysis for studying complex electrical impedance, $Z(\omega)$ and its phase angle, $\theta(\omega)$ at different frequency points, $\omega_i(\omega_i : \omega_1, \omega_2, \omega_3, ..., \omega_n)$. EIS is performed by measuring the surface potentials, $V(\omega)$ occurring from a constant current injection, $I(\omega)$ at

the boundary through a linear array of the surface electrodes attached to the sample-under-test (SUT) [3].

Bioimpedance of a sample can be measured using a two-electrode or four-electrode method. As the name implies, the two-electrode method (shown in Figure 2.1a) uses only two electrodes in series for impedance measurement. As a result, the current signal injection and voltage measurement are conducted with the same electrodes. This method suffers from electrode polarization impedance (EPI) which occurs at the electrode-tissue contact interface while the electrode is polarizable. To resolve this issue, the inter-electrode distances (IED) method was proposed [4]. Besides, electrode polarization impedance (EPI) can be minimized by introducing sufficiently high frequency at 500Hz [5]. In the four-electrode method (shown in Figure 2.1b), two separate electrode pairs are used for current injection and voltage measurements. As a result, it utilizes a linear array of four electrodes attached to the SUT. This method injects a constant amplitude current signal to the SUT through the driving (or forcing) electrodes and the frequency dependent voltage signals are measured through sensing electrodes.

2.2 Theory of Electrical Impedance Tomography

Electrical Impedance Tomography (EIT) [6-8] is a noninvasive imaging technique where the electrical conductivity, permittivity and impedance of an object is measured by an array of electrodes around it and by utilizing the measured data at domain boundary, a tomographic image of the object is reconstructed. In EIT, the electrical impedance of the object under test is

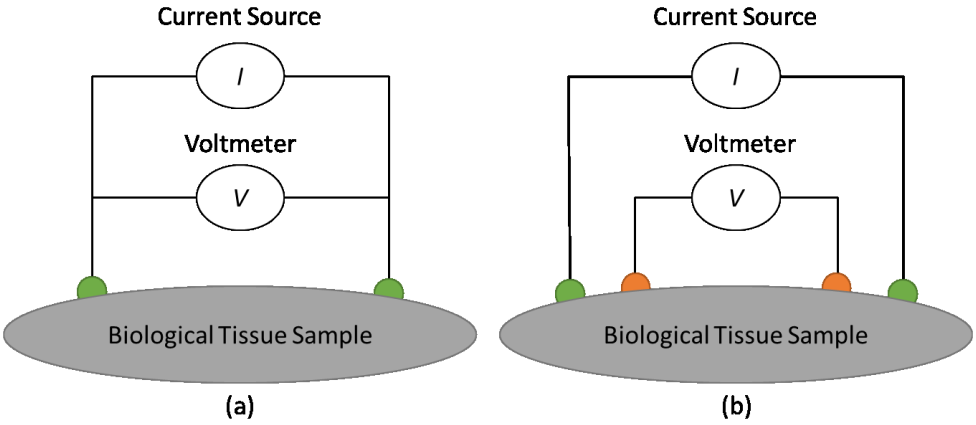

Figure 2.1 Measurement of Electrical Impedance: (a) impedance measurement using the two-electrode technique, (b) impedance measurement using the four-electrode technique

reconstructed from a set of impedance data measured at the boundary by injecting a constant voltage signal or current signal using a constant voltage source [9] or constant current source [10] using the surface electrodes [11]. The surface electrodes are attached to the boundary of the domain under test and also connected to the EIT data acquisition system (Figure 2.2). The injected signal may be of single or multiple frequencies depending on whether it is a single frequency or multi-frequency EIT system [12, 13].

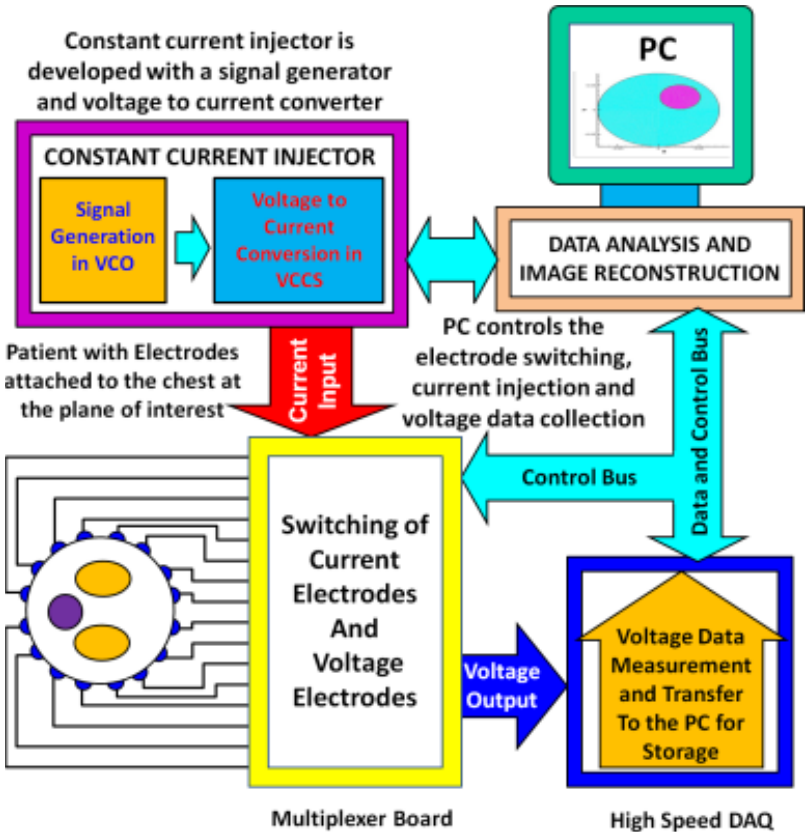

Figure 2.2 EIT data acquisition System [33]

The working principle of EIT is based on the assumption that each material possesses unique electrical properties. Exploiting this, an inhomogeneity within a homogeneous medium can be detected by using their electrical impedance. Thereby resulting electrical field (by injecting current at domain boundary) can be characterized by the distribution of material within the domain. Measured electrical potentials are fed to a nonlinear inverse algorithm to attain the unknown conductivity (resistivity) distribution. From a mathematical standpoint, the EIT problem can be divided in two categories. In a forward problem (Figure 2.3), using an initial estimation of the

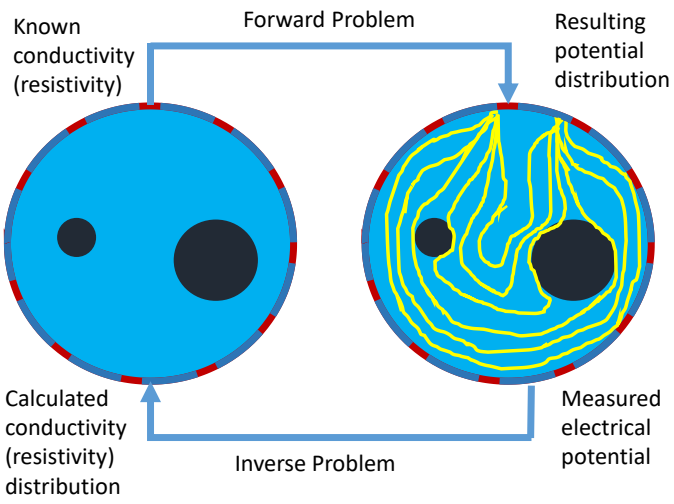

Figure 2.3 EIT forward and inverse problem

conductivity (resistivity) distribution, the electrical potentials in the boundary is calculated; while the inverse problem reconstructs the conductivity (resistivity) distribution based on the electrical potentials measured in the boundary (Figure 2.3), through the use of a mathematical procedure such as the Gauss-Newton Method.

2.3 Equivalent Circuit modeling in EIS

The EIS method provides a qualitative and quantitative analysis of the components of internal composition and microstructure of the biological material under test. It generally utilizes the electrical equivalent circuits of materials to characterize the experimental frequency response of bioimpedance. The physiological and pathological status of the biological tissues and organs can be determined by monitoring the changes in the parameters of this equivalent circuit. The resistance R and reactance X are calculated from equation (2.3) and (2.4):

$$R = |Z| \cos\theta \tag{2.3}$$

$$X = |Z| \sin\theta \tag{2.4}$$

The relationship between R and X of a complex impedance can be presented using a Nyquist plot.

Figure 2.4 shows four conventional equivalent circuit models for biological tissues. Hayden model in Figure 2.4(a), was proposed by Hayden and his co-workers [14]. It demonstrates a circuit where Re represents the extracellular resistance, Rm represents the resistance of all

membranes of all actual cells, Ri represents the intracellular resistance, and Cm represents the capacitance of all membranes of actual cells. The Hayden model has been extensively used for EIS analysis of plant and it is found to offer valuable insight into plant statuses such as ripening [15], cold injury [16] and heat injury [17]. By ignoring the cell membrane resistance, a simplified model was derived which is called simplified Hayden model [18, 19] presented in Figure 2.4(b). In order to generate better semi-eclipse response, a constant phase element (CPE) has been introduced (Figure 2.4(c)) in place of cell membrane capacitance of simplified Hayden model and it has been utilized in numerous studies [20-22] because it offers the ability to more accurate model fitting. Double-shell model (Figure 2.4(d)) is constructed with cell wall resistance (R1), cytoplasm resistance (R2), vacuole resistance (R3), plasma membrane capacitance (C1), and tonoplast capacitance (C2). In several plant investigations, the double-shell model was found useful, such as the impedance measurements conducted on nectarine fruit [23], persimmon fruit [24] and kiwifruit [25].

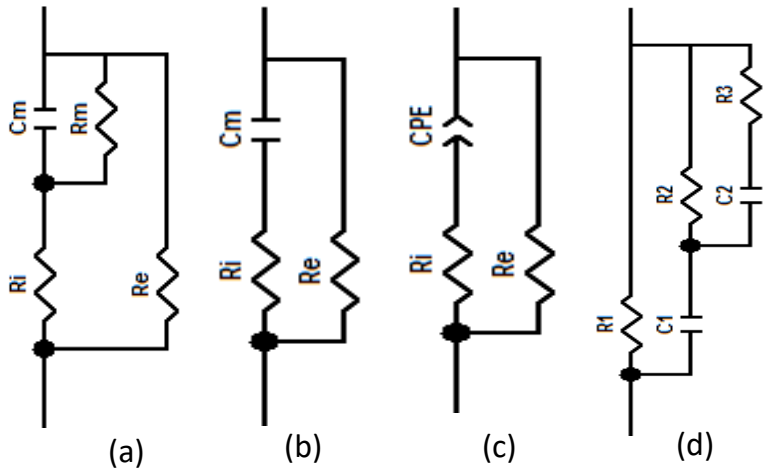

Figure 2.4 Existing equivalent circuit models for general plant tissue: (a) Hayden model [14], (b) Simplified Hayden model [18], (c) CPE-modified model [20] and (d) Double shell model [23]

2.4 Image Reconstruction in EIT: Gauss–Newton Approach

Electrical impedance imaging is a profoundly nonlinear and ill-posed inverse problem [26-28]. A minimization algorithm is used to obtain the approximate solution of an inverse problem. Minimization algorithms minimizes an objective function taking the distinction between the

experimental measurement data and the computationally anticipated data. For the most part, in inverse problems, a Gauss–Newton method based numerical approximation algorithm, called the inverse solver, looks for a least square solution [27, 28] of a minimized objective function [29, 30]. If V_m is the measured voltage matrix and f as a function mapping an E-dimensional (E is the number of element in FEM mesh) impedance distribution into a set of M (number of the measured data available) approximate measured voltage, then the Gauss–Newton algorithm [28-30] tries to find a least square solution of the minimized object function $s(\sigma)$ defined as :

$$s(\sigma) = \frac{1}{2} \| V_m - f \|^2 = \frac{1}{2} (V_m - f)^T (V_m - f) \tag{2.5}$$

Differentiating equation (2.5) w.r.t. σ, it reduces to:

$$s' = -[f]^T \, | V_m - f \| = -J^T (V_m - f) \tag{2.6}$$

where the term $J = f'$ is known as the Jacobian matrix of dimension g x h and which is defined by [31]:

$$J = [f']_{gh} = \frac{\partial f_g}{\partial \sigma_h} \tag{2.7}$$

where g = 1, 2, …, E [E = number of elements in the FEM mesh], h = 1, 2, …, M [M = (number of data measured per current projections (d)) x (number of current projections (p))].

Differentiating equation (2.6) w.r.t. σ, it reduces to:

$$s'' = \frac{\partial^2}{\partial^2 \sigma} (s) = [f']^T [f'] - [f'']^T \, | V_m - f | \tag{2.8}$$

By the inherent ill-posed nature of EIT, $[f']^T$ matrix in equation (2.8) is always ill conditioned, and hence small measurement errors will have large impacts on the solution of equation (2.8). A regularization method is incorporated to make the inverse problem well-posed by reforming the equation as:

$$s_r = \frac{1}{2} \| V_m - f \|^2 + \frac{1}{2} \lambda \| G\sigma \|^2 \tag{2.9}$$

where, s_r is the constrained least-square error of the reconstructions, G is the regularization operator and λ is a positive scalar called the regularization coefficient. Equation (2.9) can be rewritten as:

$$s_r = \frac{1}{2}(V_m - f)^T (V_m - f) + \frac{1}{2} \lambda (G\sigma)^T (G\sigma) \tag{2.10}$$

By Gauss–Newton (GN) method, the conductivity update vector reduces to:

$$\Delta\sigma = \frac{s_r'}{s_r''} = \frac{(f')^T (V_m - f) - \lambda (G)^T (G\sigma)}{(f)^T (f') - (f'')^T (V_m - f) + \lambda (G)^T G} \tag{2.11}$$

Neglecting higher order terms and replacing $G^T G$ by I (Identity matrix) equation 2.11 reduces to:

$$\Delta\sigma = (J^T J + \lambda I)^{-1} (J^T (V_m - f) - \lambda I \sigma) \tag{2.12}$$

In general, after the kth iteration (k is a positive integer), the conductivity vector can be represented as:

$$\sigma_{k+1} = \sigma_k + ([J_k]^T [J_k] + \lambda_k I)^{-1} ([J_k]^T (V_m - f)_k - \lambda_k I \sigma_k) \tag{2.13}$$

where, J_k, $(V_m - f)_k$ and λ_k are the Jacobian, the voltage difference matrix, and the regularization parameter at the kth iteration respectively.

The EIT reconstruction algorithm starts with an initial (guessed according to the prior knowledge of the background conductivity) conductivity, σ_0, and the potentials are calculated at the electrode positions. Calculated potentials are compared with the measured potential data and the J matrix is formed. The conductivity update vector, $\sigma\Delta$ is calculated using equation 2.12, and a new conductivity matrix σ_1 is formed using equation 2.13. The conductivity σ_k is modified to

$\sigma_{k+1} = \sigma_k + \sigma\Delta$ for a number of iterations using the Modified Newton–Raphson method [32]. The iteration process is continued until we obtain a specified error limit, ε , which is a function of ΔV .

References

[1] T. K. Bera, "Bioelectrical impedance methods for noninvasive health monitoring: a review," *Journal of medical engineering,* vol. 2014, pp. 1-28, 2014.

[2] J. N. M. Kreider and L. Hannapel, "Electrical impedance plethysmography: A physical and physiologic approach to peripheral vascular study," *Circulation,* vol. 2, pp. 811-821, 1950.

[3] J. R. Macdonald and E. Barsoukov, "Impedance spectroscopy: theory, experiment, and applications," *History,* vol. 1, pp. 1-13, 2005.

[4] M. Zhang and J. Willison, "Electrical Impedance Analysis in Plant Tissues11," *Journal of Experimental Botany,* vol. 42, pp. 1465-1475, 1991.

[5] T. Repo, "Seasonal changes of frost hardiness in Picea abies and Pinus sylvestris in Finland," *Canadian Journal of Forest Research,* vol. 22, pp. 1949-1957, 1992.

[6] R. H. Bayford, "Bioimpedance tomography (electrical impedance tomography)," *Annu. Rev. Biomed. Eng.,* vol. 8, pp. 63-91, 2006.

[7] M. Cheney, D. Isaacson, and J. C. Newell, "Electrical impedance tomography," *SIAM review,* vol. 41, pp. 85-101, 1999.

[8] J. G. Webster, *Electrical impedance tomography*: Taylor & Francis Group, 1990.

[9] T. Qureshi, C. Chatwin, and W. Wang, "Design of Wideband Voltage Source Having Low Output Impedance, Flexible Gain and Controllable Feedback Current for EIT Systems," in *2012 2nd International Conference on Biomedical Engineering and Technology, IPCBEE*, 2012, pp. 45-50.

[10] J. W. Lee, T. I. Oh, S. M. Paek, J. S. Lee, and E. J. Woo, "Precision constant current source for electrical impedance tomography," in *Engineering in Medicine and Biology Society, 2003. Proceedings of the 25th Annual International Conference of the IEEE*, 2003, pp. 1066-1069.

[11] A. Romsauerova, A. McEwan, L. Horesh, R. Yerworth, R. Bayford, and D. S. Holder, "Multi-frequency electrical impedance tomography (EIT) of the adult human head: initial findings in brain tumours, arteriovenous malformations and chronic stroke, development of an analysis method and calibration," *Physiological measurement,* vol. 27, p. S147, 2006.

[12] S. Kaufmann, A. Latif, W. Saputra, T. Moray, J. Henschel, U. Hofmann*, et al.*, "Multi-frequency electrical impedance tomography for intracranial applications," in *World Congress on Medical Physics and Biomedical Engineering May 26-31, 2012, Beijing, China*, 2013, pp. 961-963.

[13] N. K. Soni, A. Hartov, C. Kogel, S. P. Poplack, and K. D. Paulsen, "Multi-frequency electrical impedance tomography of the breast: new clinical results," *Physiological measurement,* vol. 25, p. 301, 2004.

[14] R. Hayden, C. Moyse, F. Calder, D. Crawford, and D. Fensom, "Electrical impedance studies on potato and alfalfa tissue," *Journal of Experimental Botany,* vol. 20, pp. 177-200, 1969.

[15] J. Juansah, I. W. Budiastra, K. Dahlan, and K. B. Seminar, "Electrical behavior of garut citrus fruits during ripening changes in resistance and capacitance models of internal fruits," *Int. J. Eng. Technol. IJET-IJENS,* vol. 12, pp. 1-8, 2012.

[16] D. Cooley and D. Evert, "Normalized electrical impedance evaluates cold injury to stem sections of'Delicious' apple," *Journal of the American Society for Horticultur,* vol. 104, pp. 561–563., 1979.

[17] M. Zhang, J. Willison, M. Cox, and S. Hall, "Measurement of heat injury in plant tissue by using electrical impedance analysis," *Canadian journal of botany,* vol. 71, pp. 1605-1611, 1993.

[18] L. Wu, Y. Ogawa, and A. Tagawa, "Electrical impedance spectroscopy analysis of eggplant pulp and effects of drying and freezing–thawing treatments on its impedance characteristics," *Journal of Food Engineering,* vol. 87, pp. 274-280, 2008.

[19] M. Zhang and J. Willison, "Electrical impedance analysis in plant tissues: the effect of freeze-thaw injury on the electrical properties of potato tuber and carrot root tissues," *Canadian Journal of Plant Science,* vol. 72, pp. 545-553, 1992.

[20] M. Itagaki, A. Taya, K. Watanabe, and K. Noda, "Deviations of capacitive and inductive loops in the electrochemical impedance of a dissolving iron electrode," *Analytical Sciences,* vol. 18, pp. 641-644, 2002.

[21] S. Ricciardi, J. Ruiz-Morales, and P. Nuñez, "Origin and quantitative analysis of the constant phase element of a platinum SOFC cathode using the state-space model," *Solid State Ionics,* vol. 180, pp. 1083-1090, 2009.

[22] S. Skale, V. Doleček, and M. Slemnik, "Substitution of the constant phase element by Warburg impedance for protective coatings," *Corrosion science,* vol. 49, pp. 1045-1055, 2007.

[23] F. R. Harker and J. H. Maindonald, "Ripening of nectarine fruit (changes in the cell wall, vacuole, and membranes detected using electrical impedance measurements)," *Plant physiology,* vol. 106, pp. 165-171, 1994.

[24] F. R. Harker and S. K. Forbes, "Ripening and development of chilling injury in persimmon fruit: an electrical impedance study," *New Zealand Journal of Crop and Horticultural Science,* vol. 25, pp. 149-157, 1997.

[25] A. D. Bauchot, F. R. Harker, and W. M. Arnold, "The use of electrical impedance spectroscopy to assess the physiological condition of kiwifruit," *Postharvest Biology and technology,* vol. 18, pp. 9-18, 2000.

[26] K.-H. Cho, S. Kim, and Y.-J. Lee, "A fast EIT image reconstruction method for the two-phase flow visualization," *International communications in heat and mass transfer,* vol. 26, pp. 637-646, 1999.

[27] B. M. Graham, "Enhancements in Electrical Impedance Tomography (EIT) image reconstruction for three-dimensional lung imaging," University of Ottawa (Canada), 2007.

[28] T. Yorkey, "Comparing reconstruction methods for electrical impedance tomography [Ph. D. thesis]," *University of Wisconsin, Madison,* 1986.

[29] S. R. Arridge, "Optical tomography in medical imaging," *Inverse problems,* vol. 15, p. R41, 1999.

[30] S. K. Biswas, K. Rajan, and R. Vasu, "Interior photon absorption based adaptive regularization improves diffuse optical tomography," in *Second International Conference on Digital Image Processing*, 2010, p. 754611.

[31] C. J. Grootveld, "Measuring and modeling of concentrated settling suspensions using electrical impedance tomography," 1998.

[32] T. K. Bera and J. Nagaraju, "A FEM-based forward solver for studying the forward problem of electrical impedance tomography (EIT) with a practical biological phantom," in *Advance Computing Conference, 2009. IACC 2009. IEEE International*, 2009, pp. 1375-1381.

[33] T. K. Bera, "Applications of Electrical Impedance Tomography (EIT): A Short Review," in *IOP Conference Series: Materials Science and Engineering*, 2018, p. 012004.

Chapter 3 – Model of Dehydration and Assessment of Moisture Content on Onion Using EIS

The content of this chapter comes from an original manuscript titled M. Islam, K. Wahid, A. Dinh and P. Bhowmik, "Model of Dehydration and Assessment of Moisture Content on Onion Using ElS," accepted and to appear in *Journal of Food Science and Technology*. The manuscript is modified and reorganized according to the writing style of this thesis. The manuscript is written by me (M. Islam) under the supervision of K. Wahid, A. Dinh and P. Bhowmik. Reviewing the literature, designing and performing the experiment and analysis of result were done by me (M. Islam) under the supervision of K. Wahid, A. Dinh and P. Bhowmik.

In this chapter, a nondestructive electrical impedance spectroscopy technique is used to monitor the physiological status of onion undergoing dehydration. An equivalent circuit model is proposed to track the physiological changes nondestructively and noninvasively. The model shows a good agreement with experimental ground-truth data. In addition, the prospect of electrical impedance spectroscopy is explored to offer nondestructive alternative for assessing moisture content. The proposed approach can serve as an easily accessible alternative tool for storage period quality assessment of onion.

Model of Dehydration and Assessment of Moisture Content on Onion Using EIS

Monzurul Islam[1], Khan Wahid[1], Anh Dinh[1], Pankaj Bhowmik[2]

[1] Department of Electrical and Computer Engineering, University of Saskatchewan, Saskatoon S7N 5A2, Canada.

[2]National Research Council, Saskatoon, Saskatchewan, Canada.

Correspondence should be addressed to Monzurul Islam; moi352@mail.usask.ca

Abstract

Onion is perishable and thereby subject to drying during unrefrigerated storage. Its moisture content is important to ensure optimum quality in storage. To track and analyze the dynamics of natural dehydration in onion and also to assess its moisture content, noninvasive and nondestructive methods are preferred. One of them is known as Electrical Impedance Spectroscopy (or EIS in short). In the first phase of our experiment, we have used EIS, where we apply alternating current with multiple frequency to the object (onion in this case) and generate impedance spectrum which is used to characterize the object. We then develop an equivalent electrical circuit representing onion characteristics using a computer assisted optimization technique that allows us to monitor the response of onion undergoing natural drying for a duration of three weeks. The developed electrical model shows better congruence with the impedance data measured experimentally when compared to other conventional models for plant tissue with a mean absolute error of 0.42% and root mean squared error of 0.55%. In the second phase of our experiment, we attempted to find a correlation between the previous impedance data and the actual moisture content of the onions under test (measured by weighing) and developed a mathematical model. This model will provide an alternative tool for assessing the moisture content of onion nondestructively. Our model shows excellent correlation with the ground truth data with a deterministic coefficient of 0.977, root mean square error of 0.030 and sum of squared error of 0.013. Therefore, our two models will offer plant scientists the ability to study the physiological status of onion both qualitatively and quantitatively.

Keywords: Electrical Impedance Spectroscopy, Bioimpedance, Biological tissues, Dehydration, Onion, Moisture content.

3.1 Introduction

Onion represents the third largest fresh vegetable industry after potato and tomato, and is one of the highly consumed vegetable in the world [1]. Onion, being perishable, is subject to deterioration and post-harvest loss during storage. This storage loss results in a substantial drop of market value and food quality of onion. Quality standard organizations such as, Agriculture and Agri-Food Canada and Canadian Food Inspection Agency demand proper control and maintenance of food quality during storage. Therefore, quality maintenance during storage of onion is a major thrust area of food processing and preservation for a long time. The storage loss of onion is mainly caused by rotting, sprouting and physiological weight loss. During unrefrigerated storage at ambient temperature, onion loses moisture content which leads to loss of weight. Therefore, understanding of the dynamics of onion drying and the assessment of its moisture content is critical to ensuring optimum quality to onion storage. Currently used conventional evaporation methods (forced draft oven, vacuum oven, and microwave oven) for moisture content determination are often destructive, time consuming, and may cause unwanted chemical decomposition of the samples. Microwave heating , which is comparatively faster than conventional and vacuum oven drying methods, is expensive and destructive in nature [2]. Nondestructive methods like Magnetic Resonance Imaging (MRI) [3] is ideal for assessing water distribution through food products. This method requires separation of signal of water proton from that of fat proton which is still a challenging task. And MRI is limited by the factors such as high cost and processing complexity. Hyperspectral imaging can effectively assess moisture content but it also suffers from constrains like cost and processing [4]. Therefore, it is essential to expand current technologies from different viewpoints.

Developing a relation between food qualities and engineering properties of food is the main challenge of today's food engineering. The electrical properties of food are found to be related to the food quality and can be utilized to reveal the physiological properties [5]**.** Electrical sensing technology is found to uncover the fundamental attributes in plants and vegetables and to follow physiological progressions due to environmental impacts. Electrical Impedance Spectroscopy

(EIS) is one of the methods of measuring electrical characteristics with a small amplitude sine wave voltage (or current). Impedance Spectrum can be determined using a multi-frequency impedance analyzer by observing the electrical response of tissues to the passage of the external power [6]. EIS can allow insight into the physiological and pathological information on biological tissues and organs [5]. Moreover, it is found to provide comprehensive qualitative and quantitative analyses of the inner components of the composition and microstructure of the subject under test.

Considering the benefits of EIS as an accessible and nondestructive tool, in this paper, we propose to use it to understand the mechanisms of dehydration and to assess moisture content of onion. This work mainly focuses on two aspects: first to generate an equivalent electrical circuit to simulate the electrical characteristics of onion during natural dehydration process. Secondly, to develop a mathematical model to assess the moisture content of onion nondestructively. The paper is organized as follows: related past works on the application of EIS is presented in Section 3.2. Experimental methods and materials are illustrated in section 3.3. The results are presented and discussed in Section 3.4. Finally the study is concluded in section 3.5.

3.2 Literature Review

Impedance sensing technology, especially EIS, has been shown useful in food quality and stability monitoring over the last decades. In order to assess the freshness of banana, EIS investigation was performed during different ripening state [7]**.** By attaching Ag/AgCl electrode and injecting a small amount of current, impedance responses are measured by an Impedance Analyzer over a frequency range of 50Hz to 1MHz. The impedance magnitude, phase angle, real and imaginary part varied markedly with the alteration of ripening state. Apples properties during 21 days of aging were monitored using EIS to provide information about the physical properties of apple [8]. Two different analytical techniques for assessment of the changes of apples' properties during aging time were proposed. The first one is a single measurement in the low frequency range (around 100Hz) and the second one is multi-frequency argand plot on a complex plane. The results propose that alteration in observed EIS can be attributed to the changes in the relative moisture content of the apple. In order to evaluate the nitrate level in lettuce, Muñoz-Huerta, et al. [9] executed bio-impedance measurements over 30 lettuce plants, treated with different nutrient solutions. Experimental results led to the conclusion that impedance increase proportionally with nitrogen content. These results support the hypothesis that EIS technique can

be an effective tool to monitor nitrogen and other ions in plant tissue. Some major factors that influence dielectric properties of agricultural and biological materials are salt content, moisture content, and the state of moisture (frozen, free or bound). Many studies on dielectric properties of vegetables and fruits have been reported for different frequency ranges, temperatures, and moisture contents. The experimental results of the moisture content of material undergoing microwave drying were in congruence with the predictions of the proposed model [10]**.** Kertész, et al. [11] utilized EIS to measure electrical response of carrot slice during drying by HP 4284A and 4285A precision LCR meters in the frequency range from 30Hz to 1MHz and from 75kHz to 30MHz, respectively, at a voltage of 1V. By measuring the weight of the samples with a with a DenverSI-603 electronic analytical and precision balance, the moisture content was calculated on wet basis. Moisture content was found to decrease according to a polynomial function and alteration of impedance during drying showed good correlation with change in moisture content. Ando, et al. [12] investigated EIS to explore the changes in the cell physiological status of potato tissues during hot air drying at 50–80^{0}C. At early drying stage, from the initial moisture content to moisture content of 1.0 (dry basis), the modified Hayden model was found to be useful to describe the impedance characteristics. Thus, EIS technique was found to offer a great insight into physiology of fruits and vegetables undergoing natural drying process.

3.3 Materials and Methods

Our experiment is divided into several steps. First of all, we measured the actual moisture content of onion by weighing it for a duration of three weeks. At the same time, we use EIS tool to measure the electrical response of the onion sample. Then, we generate an equivalent circuit model using the impedance-frequency response. In the last stage, the impedance responses are correlated with their corresponding moisture contents.

3.3.1 Sample Preparation

In our experiment, we used yellow onion (Allium cepa) that were collected randomly from a local supermarket ‘Sobeys’ in Saskatoon, Canada. A total number of 10 onion samples with varying size and weight (ranging from 75 to 96 gram) were chosen. During the three weeks period, these samples were kept in room temperature (roughly around 20°C) with a relative humidity of 40%.

3.3.2 Measurement of Moisture Content

During storage, onion is subject to deterioration as it loses its weight due to natural drying [13]. This weight loss is measured and recorded daily during the period of experiment. A high precision milligram balances with 0.001g accuracy (Intelligent-Lab PMW-320) was used. The moisture content relative to solid content, M, in onion is calculated from equation (3.1)

$$M = \frac{m_t - s \times m_o}{s \times m_o} \tag{3.1}$$

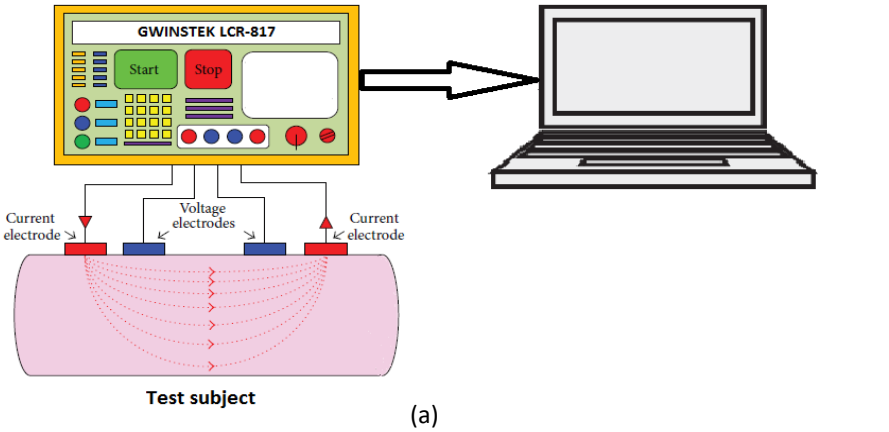

(a)

(b)

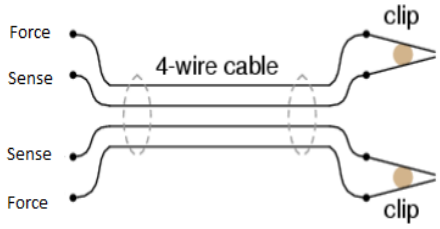

(c)

Figure 3.1 (a) Schematic illustration for the EIS measurement system of onion, (b) Experimental device for electrical impedance spectroscopy measurement of onion, (c) 4-wire Kelvin clips for impedance measurement.

where, m_o is the initial weight of the sample, s is the initial percentage of solid content in the sample (which is assumed to be 13% [14]), m_t is the weight of the sample at time, t.

3.3.3 Measurement of EIS

Impedance measurement on onion samples was carried out with a high precision LCR meter (GWINSTEK LCR-817). The LCR device has a built-in signal generator and works in the frequency range from 12 Hz to 10 kHz with 489 steps and 0.05% accuracy. Due to its high accuracy and versatility, the device is suitable for material and bio-impedance measurements. For impedance measurements in our experiment, we used a 1V p-p generator voltage and scanned 27 spot frequencies with frequency intervals between 0.5 KHz to 10 KHz. The experimental setup for EIS measurement is shown in Figure 3.1a. Figure 3.1b shows the experimental device for our impedance measurement system where Kelvin method was used. In regular "alligator" style clips, both halves of the jaw are joined at the hinge point and electrically common to each other. In Kelvin method, a single clip (LCR-06A) is used that contains a sense-force electrode pair isolated at hinge point as shown in Figure 3.1c.

3.3.4 Equivalent Circuit Modeling

The EIS method provides a qualitative and quantitative analysis of the components of internal composition and microstructure of the biological material under test. It generally utilizes the electrical equivalent circuits of materials to characterize the experimental frequency response of bioimpedance. The physiological and pathological status of the biological tissues and organs can be determined by monitoring the changes in parameters of this equivalent circuit. The resistance R and reactance X are calculated from equation (3.2) and (3.3):

$$R = |Z| \cos\theta \tag{3.2}$$

$$X = |Z| \sin\theta \tag{3.3}$$

The relationship between R and X of a complex impedance can be presented using a Nyquist plot. Figure 3.2 shows four conventional equivalent circuit models for biological tissues. Hayden model in Figure 3.2a, was proposed by Hayden and his co-workers [15]. It demonstrates a circuit where Re represents the extracellular resistance, Rm represents the resistance of all membranes of all

actual cells, Ri represents the intracellular resistance, and Cm represents the capacitance of all membranes of actual cells. The Hayden model has been extensively used for EIS analysis of plant and it is found to offer valuable insight into plant status such as ripening [16], cold injury [17] and heat injury [18]. By ignoring the cell membrane resistance, a simplified model was derived which is called simplified Hayden model [19, 20] presented in Figure 3.2b. In order to generate better semi-eclipse response, a constant phase element (CPE) has been introduced (Figure 3.2c) in place of cell membrane capacitance of simplified Hayden model and it has been utilized in numerous studies [21-23] because it offers the ability to more accurate model fitting. Double-shell model (Figure 3.2d) is constructed with cell wall resistance (R1), cytoplasm resistance (R2), vacuole resistance (R3), plasma membrane capacitance (C1), and tonoplast capacitance (C2). In several plant investigations, the double-shell model was found useful, such as the impedance measurements conducted on nectarine fruit [24], persimmon fruit [25] and kiwifruit [26].

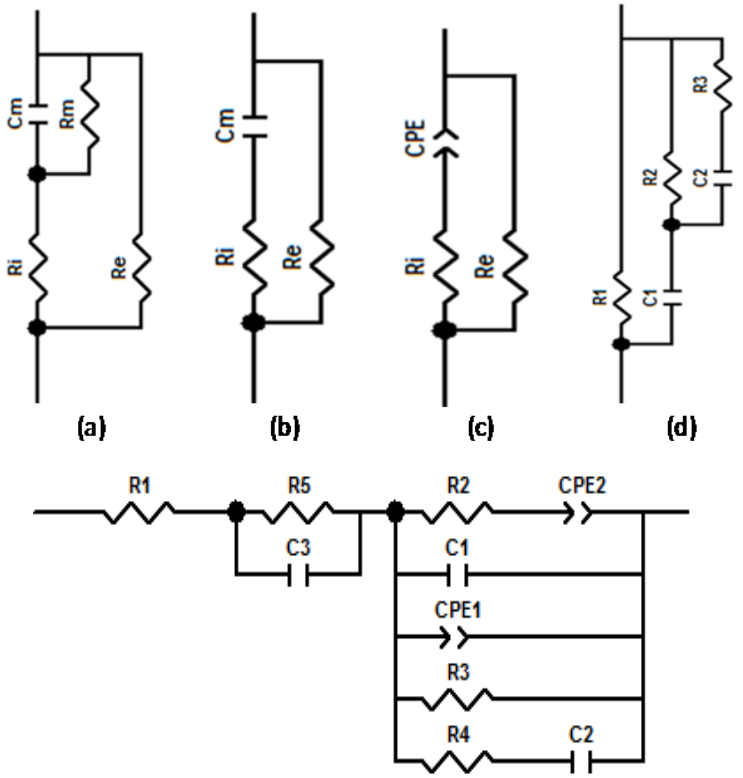

Figure 3.2 Existing equivalent circuit models for general plant tissue: (a) Hayden model [15], (b) Simplified Hayden model [19], (c) CPE-modified model [21], (d) Double shell model [24], and (e) Our proposed model for onion dehydration.

To visualize the dehydration of onion over a period of 21 days, our work has proposed an electrical model that showed excellent agreement with the experimental data. Based on this model, physiological change of onion during drying by means of electrical response can be demonstrated. The optimization of circuit parameters of this equivalent circuit model has been achieved by 'Nelder Mead Simplex' curve fitting algorithm in 'EIS Spectrum Analyzer' software. The model is later illustrated and compared with the conventional ones in the following section.

3.4 Result and Discussion

3.4.1 Dependence of Bioimpedance on Frequency and Dehydration

As water plays a vital role in all processes in biomaterials [27], it is expected that significant change will occur in impedance with the dehydration process in onions. The EIS studies conducted for different onion samples for three weeks showed that at a particular frequency, the onion impedance gradually increases throughout the experiment as drying time proceeds (Figure 3.3a). Moreover, for a particular day, impedance decreased significantly from low to high frequency and this phenomenon is termed as dispersion. Figure 3.3b shows that the phase angle of onion impedance varies with frequency throughout the drying period. In similar fashion with impedance magnitude, the real part of the onion impedance increases with dehydration period at a particular frequency (Figure 3.3c). However, at a particular day, the real part of the onion impedance decreases from low to high frequency regions (Figure 3.3c). Figure 3.3d shows that the imaginary part of onion impedance varies significantly as the drying period proceeds. This phenomenon happens due to the variations in reactive part in the onion impedance during dehydration.

At lower frequency, the electrical current flows only through extracellular fluids which act as electrolytes and have relatively high resistance. The cell membrane exert extreme high capacitance at low frequency and that is why electrical current cannot pass through and only flows through the extracellular fluid. At high frequency, cell membrane capacitance reduces significantly and current flows through intracellular fluid, which has relatively low resistance. This is how impedance magnitude declines markedly from low to high frequency area of impedance spectra. This phenomenon resulting from cell structures in biological tissue is known as β dispersion [28]. Again, to maintain the structural and functional integrity of biological membranes, water content plays a vital role [29]**.** The movement of the ions during drying causes the changes in cell

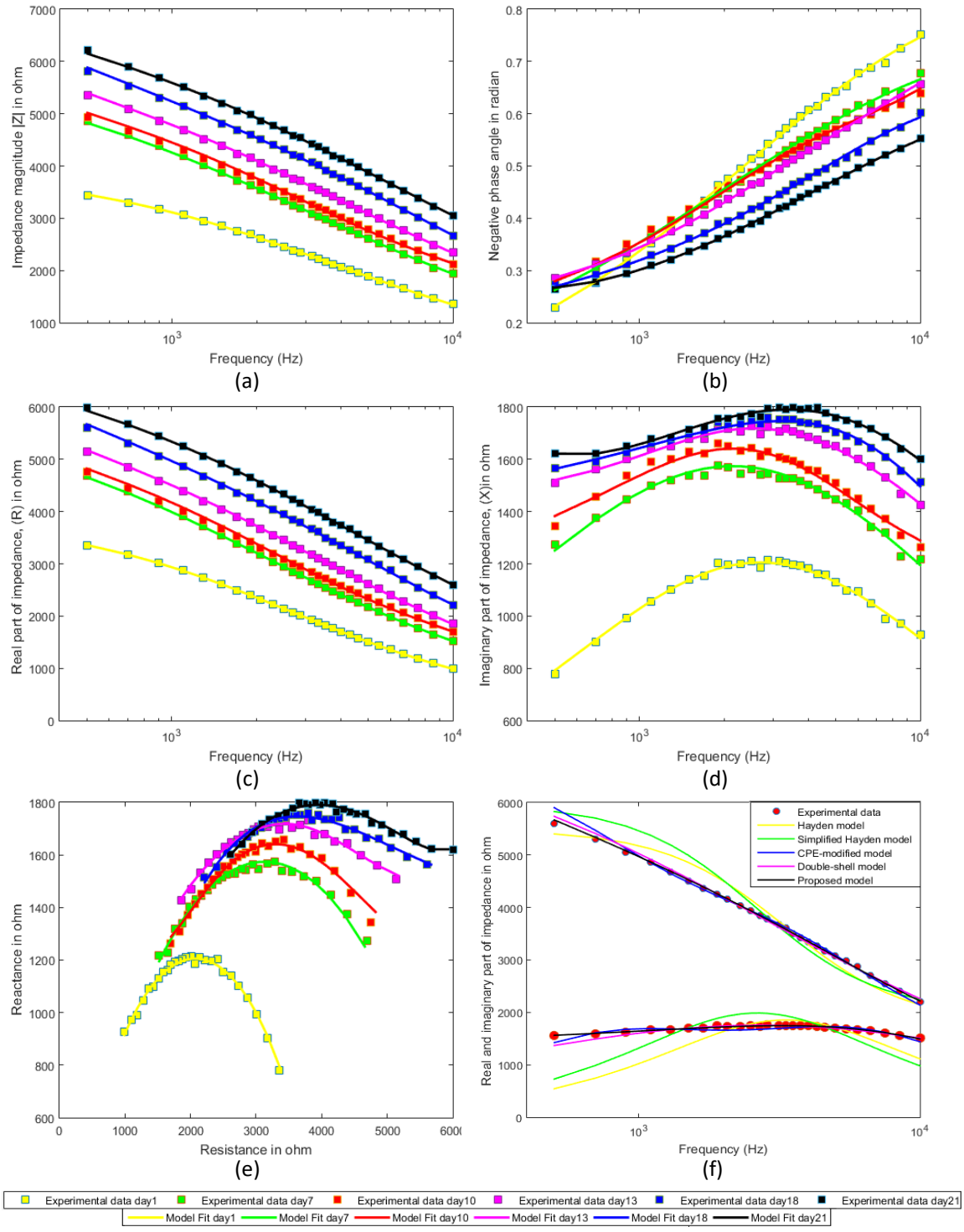

Figure 3.3 Impedance response of onion during dehydration: (a) Impedance vs. Frequency plot, (b) Phase angle vs. Frequency plot, (c) Real part of impedance vs. Frequency plot, (d) Imaginary part of impedance vs. Frequency plot (e) Reactance vs. Resistance plot (Nyquist plot), and (f) Experimental fit and simulated fit of all models at day 18.

membrane capacitance. As shown in Figure 3.3a, at a particular frequency, impedance of onion increased gradually with drying. So it can be concluded that the disruption of cell membrane of onion with drying process leads to increase of cell membrane capacitance which results in an increase of overall impedance of onion. and current flows through intracellular fluid, which has relatively low resistance. This is how impedance magnitude declines markedly from low to high frequency area of impedance spectra. This phenomenon resulting from cell structures in biological tissue is known as β dispersion [28]. Again, to maintain the structural and functional integrity of biological membranes, water content plays a vital role [29]**.** The movement of the ions during drying causes the changes in cell membrane capacitance. As shown in Figure 3.3a, at a particular frequency, impedance of onion increased gradually with drying. So it can be concluded that the disruption of cell membrane of onion with drying process leads to increase of cell membrane capacitance which results in an increase of overall impedance of onion.

Furthermore, the experimental results over 3 weeks were modeled with the help of equivalent circuit method to describe onion tissue features using electrical circuit scheme. The circuit element and connections are dependent on experimental data and their curve fittings. In this concern, Nyquist plots, representing real part of impedance, R versus imaginary part of impedance, X dependences, were constructed at first. Nyquist plots for an onion undergoing drying are presented in Figure 3.3e. For quantifying the changes of impedance characteristics, EIS data were analyzed in term of equivalent model. The equivalent electrical circuit of onion during dehydration is shown in Figure 3.2e.

To extract the parameters that cause best agreement between model spectrum and measured spectrum, 'Nelder Mead Simplex' algorithm was used. The equivalent circuit modeling and curve fitting were performed in 'EIS Spectrum Analyzer' software. Starting from the given initial estimates, the algorithm makes changes in the parameters and evaluates the resulting fits. Iterations continue until the goodness of fit exceeds a predefined acceptance criterion. The equivalent electrical circuit parameters (R for resistance, C for Capacitance, and P for pre-exponential factor of constant phase element, CPE and n for CPE exponent) of onion during dehydration are obtained from non-linear curve fitting. As our experiment was performed on yellow onion (Allium cepa), the proposed model of onion may change from variety to variety and so impedance studies on the other onion variety could be conducted in future studies.

To assess the goodness of curve fitting, it is a common practice to measure mean absolute percentage error and root mean squared percentage error. So to evaluate the performance of our analytical model, the aforementioned indices of goodness of fit were calculated. It becomes evident from Table 3.1 that the proposed model outperforms the other conventional models in terms of performance parameters. The mean absolute percentage error is as low as 0.42% for real part and 0.48% for imaginary part and root mean squared percentage error is 0.55% for real part and 0.58% for imaginary part. Figure 3.3f also demonstrates that the proposed model is in better congruence with experimental data compared to the conventional ones.

3.4.2 Estimation of Moisture content Using Bioimpedance

The moisture content variation for different storage times during drying is shown in Figure 3.4a. During the entire experimental period, the moisture content decreases as drying time proceeds and it creates alteration in electrical conductivity and bioimpedance in onion. Comparing the results from Figure 3.3a and Figure 3.4a, it can be assumed that moisture content and bioimpedance can be connected and variation of impedance could be attributed to the decrease of moisture content.

The dependencies between impedance magnitude and relative moisture content on onion are disclosed in Figure 3.4b, 3.4c, 3.4d and 3.4e. All of the sample onions show the same phenomenon that the impedance magnitude at a particular frequency increase over drying period as moisture content decreases. The correlation between impedance and moisture content is found to be relatively high at higher frequencies and it is possibly due to the fact that alternating current can penetrate the sample more deeply only at high frequency. The current can flow through intercellular fluid if frequencies at β-dispersion region are chosen. If frequencies lower than β-dispersion region are selected, the current can only flow through the extracellular space [30].

Degree one polynomial equations for determination of moisture content in onion at various frequencies are shown in Table 3.2. By reviewing the deterministic coefficients (R^2), Root Mean Square Error (RMSE) and Sum of Squared Error (SSE), those equations are found to offer fairly good estimations. The lowest correlation occurred at a frequency of 0.5 kHz and the highest correlation occurred at a frequency of 10 KHz. According to the values of deterministic coefficient, root mean square error and sum of squared error, the best correlation was found at a frequency of

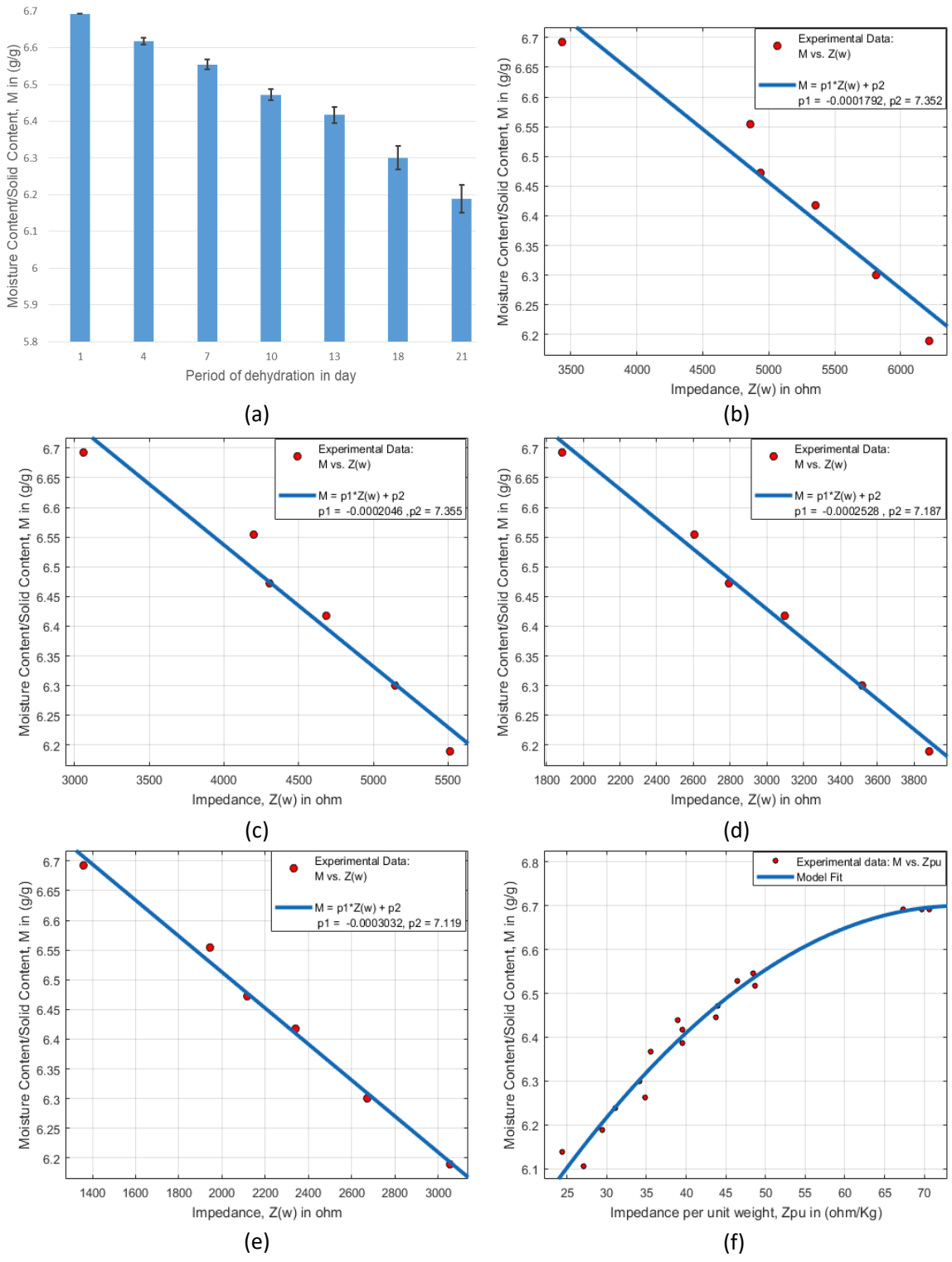

Figure 3.4 Moisture content variations: (a) at different time of drying period, (b) Correlation with impedance at 0.5 KHz, (c) Correlation with impedance at 1.1 KHz, (d) Correlation with impedance at 5 KHz, (e) Correlation with impedance at 10 KHz, and (f) Estimation of relative moisture content using impedance per unit weight.

10 KHz which is characterized by the highest deterministic coefficient ($R^2 = 0.994$) , lowest Root Mean Square Error (RMSE = 0.016) and lowest Sum of Squared Error (SSE = 0.001).

Moreover, to compensate the variation of size and weight for different onion samples, we expressed the impedance (at 10 KHz) in per unit weight and investigated the correlation with corresponding moisture content as shown in Figure 3.4f. The model (at 10 KHz) derived from degree two polynomial curve fitting is shown in equation (3.4).

$$M(Zpu) = -0.0002442Zpu^2 + 0.03636Zpu + 5.346 \quad (3.4)$$

where, $M(Zpu)$ is relative moisture content in g/g and Zpu is impedance per unit weight in Ohm/Kg. The proposed model shows fairly good estimates with a deterministic coefficient of 0.977, root mean square error of 0.030 and sum of squared error of 0.013.

So the performance parameters of the corresponding model proves that electrical impedance has really high potential for estimating moisture content of onion. This model can be used as a reference model for assessing moisture of onion during post-harvest storage. Due to its easily accessible and nondestructive nature, it can be used as an alternative to existing tools to estimate the relative moisture content value of onion undergoing natural drying.

Table 3.1 Comparison of fitting performance of different models

Model	**Mean absolute error (%)**		**Root mean squared error (%)**	
	Real Part of Z	**Imaginary Part of Z**	**Real Part of Z**	**Imaginary Part of Z**
Hayden [15]	4.52	14.23	5.14	21.77
Simplified Hayden [19]	5.81	14.46	6.57	18.89
Double-Shell [21]	1.16	2.55	1.63	3.17
CPE-modified [24]	1.13	1.34	1.30	2.85
Proposed	0.42	0.48	0.55	0.58

In future studies, low cost impedance sensor such as AD5933 is to be integrated to the system to replace comparatively expensive LCR meter used in this study. Future works also include the development of an automated moisture content monitoring system based on EIS by

combining environment controller, wireless communication module and portable monitoring device.

Table 3.2 Estimation of relative moisture content and corresponding performance indices

Frequency (kHz)	Model	SSE	R-Square	RMSE
0.5	M = p1*Z(w) + p2 p1 = -0.0001792, p2 = 7.352	0.010	0.935	0.051
1.1	M = p1*Z(w) + p2 p1 = -0.0002046 , p2 = 7.355	0.007	0.959	0.041
5	M = p1*Z(w) + p2 p1 = -0.0002528 , p2 = 7.187	0.001	0.990	0.020
10	M = p1*Z(w) + p2 p1 = -0.0003032, p2 = 7.119	0.001	0.994	0.016

3.5 Conclusion

In this paper, electrical impedance spectroscopy, a nondestructive technique, has been utilized to monitor the physiological status of onion undergoing dehydration. Electrical impedance parameters are found to be sensitive to the alteration of water content in onion. Moreover, to track the physiological changes nondestructively and noninvasively, an equivalent circuit model has been proposed that show good agreement with experimental results. In addition, the prospect of electrical impedance spectroscopy to offer nondestructive alternative for assessing moisture content on onion has been explored. Proposed approach can serve as an easily accessible alternative tool for storage period quality assessment of onion.

References

[1] J. Mitra, S. Shrivastava, and P. Rao, "Onion dehydration: a review," *Journal of food science and technology,* vol. 49, pp. 267-277, 2012.

[2] W. Canet, "Determination of the moisture content of some fruits and vegetables by microwave heating," *Journal of Microwave Power and Electromagnetic Energy,* vol. 23, pp. 231-235, 1988.

[3] J. Irudayaraj and S. Gunasekaran, "Optical methods: visible, NIR, and FTIR spectroscopy," *Nondestructive food evaluation techniques to analyze properties and quality. New York: Marcel Dekker. p,* pp. 1-2, 2001.

[4] F. Raponi, R. Moscetti, D. Monarca, A. Colantoni, and R. Massantini, "Monitoring and Optimization of the Process of Drying Fruits and Vegetables Using Computer Vision: A Review," *Sustainability,* vol. 9, p. 2009, 2017.

[5] D. El Khaled, N. Castellano, J. Gazquez, R. G. Salvador, and F. Manzano-Agugliaro, "Cleaner quality control system using bioimpedance methods: a review for fruits and vegetables," *Journal of Cleaner Production,* vol. 140, pp. 1749-1762, 2017.

[6] T. K. Bera, "Bioelectrical impedance methods for noninvasive health monitoring: a review," *Journal of medical engineering,* vol. 2014, pp. 1-28, 2014.

[7] A. Chowdhury, T. Bera, D. Ghoshal, and B. Chakraborty, "Studying the electrical impedance variations in banana ripening using electrical impedance spectroscopy (EIS)," in *Proceedings of the 2015 Third International Conference on Computer, Communication, Control and Information Technology (C3IT), Hooghly, 2015, 1-4*, 2015, pp. 1-4.

[8] T. Yovcheva, E. Vozáry, I. Bodurov, A. Viraneva, M. Marudova, and G. Exner, "Investigation of apples aging by electric impedance spectroscopy," *Bulg. Chem. Commun,* vol. 45, pp. 68-72, 2013.

[9] R. F. Muñoz-Huerta, A. d. J. Ortiz-Melendez, R. G. Guevara-Gonzalez, I. Torres-Pacheco, G. Herrera-Ruiz, L. M. Contreras-Medina*, et al.*, "An analysis of electrical impedance measurements applied for plant N status estimation in lettuce (Lactuca sativa)," *Sensors,* vol. 14, pp. 11492-11503, 2014.

[10] M. Hemis, R. Choudhary, and D. G. Watson, "A coupled mathematical model for simultaneous microwave and convective drying of wheat seeds," *Biosystems engineering,* vol. 112, pp. 202-209, 2012.

[11] Á. Kertész, Z. Hlaváčová, E. Vozáry, and L. Staroňová, "Relationship between moisture content and electrical impedance of carrot slices during drying," *International Agrophysics,* vol. 29, pp. 61-66, 2015.

[12] Y. Ando, K. Mizutani, and N. Wakatsuki, "Electrical impedance analysis of potato tissues during drying," *Journal of Food Engineering,* vol. 121, pp. 24-31, 2014.

[13] K. Alabi, A. Olaniyan, and M. Odewole, "Characteristics of Onion under Different Process Pretreatments and Different Drying Conditions," *J Food Process Technol,* vol. 7, pp. 1-7, 2016.

[14] L. Abhayawick, J. Laguerre, V. Tauzin, and A. Duquenoy, "Physical properties of three onion varieties as affected by the moisture content," *Journal of Food Engineering,* vol. 55, pp. 253-262, 2002.

[15] R. Hayden, C. Moyse, F. Calder, D. Crawford, and D. Fensom, "Electrical impedance studies on potato and alfalfa tissue," *Journal of Experimental Botany,* vol. 20, pp. 177-200, 1969.

[16] J. Juansah, I. W. Budiastra, K. Dahlan, and K. B. Seminar, "Electrical behavior of garut citrus fruits during ripening changes in resistance and capacitance models of internal fruits," *Int. J. Eng. Technol. IJET-IJENS,* vol. 12, pp. 1-8, 2012.

[17] D. Cooley and D. Evert, "Normalized electrical impedance evaluates cold injury to stem sections of'Delicious' apple," *Journal of the American Society for Horticultur,* vol. 104, pp. 561–563., 1979.

[18] M. Zhang, J. Willison, M. Cox, and S. Hall, "Measurement of heat injury in plant tissue by using electrical impedance analysis," *Canadian journal of botany,* vol. 71, pp. 1605-1611, 1993.

[19] L. Wu, Y. Ogawa, and A. Tagawa, "Electrical impedance spectroscopy analysis of eggplant pulp and effects of drying and freezing–thawing treatments on its impedance characteristics," *Journal of Food Engineering,* vol. 87, pp. 274-280, 2008.

[20] M. Zhang and J. Willison, "Electrical impedance analysis in plant tissues: the effect of freeze-thaw injury on the electrical properties of potato tuber and carrot root tissues," *Canadian Journal of Plant Science,* vol. 72, pp. 545-553, 1992.

[21] M. Itagaki, A. Taya, K. Watanabe, and K. Noda, "Deviations of capacitive and inductive loops in the electrochemical impedance of a dissolving iron electrode," *Analytical Sciences,* vol. 18, pp. 641-644, 2002.

[22] S. Ricciardi, J. Ruiz-Morales, and P. Nuñez, "Origin and quantitative analysis of the constant phase element of a platinum SOFC cathode using the state-space model," *Solid State Ionics,* vol. 180, pp. 1083-1090, 2009.

[23] S. Skale, V. Doleček, and M. Slemnik, "Substitution of the constant phase element by Warburg impedance for protective coatings," *Corrosion science,* vol. 49, pp. 1045-1055, 2007.

[24] F. R. Harker and J. H. Maindonald, "Ripening of nectarine fruit (changes in the cell wall, vacuole, and membranes detected using electrical impedance measurements)," *Plant physiology,* vol. 106, pp. 165-171, 1994.

[25] F. R. Harker and S. K. Forbes, "Ripening and development of chilling injury in persimmon fruit: an electrical impedance study," *New Zealand Journal of Crop and Horticultural Science,* vol. 25, pp. 149-157, 1997.

[26] A. D. Bauchot, F. R. Harker, and W. M. Arnold, "The use of electrical impedance spectroscopy to assess the physiological condition of kiwifruit," *Postharvest Biology and technology,* vol. 18, pp. 9-18, 2000.

[27] D. Jamaludin, S. A. Aziz, D. Ahmad, and H. Z. Jaafar, "Impedance analysis of labisia pumila plant water status," *Information Processing in Agriculture,* vol. 2, pp. 161-168, 2015.

[28] R. Pethig and D. B. Kell, "The passive electrical properties of biological systems: their significance in physiology, biophysics and biotechnology," *Physics in Medicine & Biology,* vol. 32, p. 933, 1987.

[29] J. H. Crowe and L. M. Crowe, "Induction of anhydrobiosis: membrane changes during drying," *Cryobiology,* vol. 19, pp. 317-328, 1982.

[30] D. Dean, T. Ramanathan, D. Machado, and R. Sundararajan, "Electrical impedance spectroscopy study of biological tissues," *Journal of electrostatics,* vol. 66, pp. 165-177, 2008.

Chapter 4 – Assessment of Ripening Degree of Avocado by Electrical Impedance Spectroscopy and Support Vector Machine

Published as M. Islam, K. Wahid and A. Dinh, "Assessment of Ripening Degree of Avocado by Electrical Impedance Spectroscopy and Support Vector Machine," *Journal of Food Quality, 2018.* Volume 2018, Article ID 4706147, https://doi.org/10.1155/2018/4706147. The manuscript is modified and reorganized according to the writing style of this thesis. The manuscript is written by me (M. Islam) under the supervision of K. Wahid, A. Dinh. Reviewing the literature, designing and performing the experiment and analysis of result were done by me (M. Islam) under the supervision of K. Wahid and A. Dinh.

In this chapter, the feasibility of electrical impedance spectroscopy, a nondestructive technique is explored to assess the ripening degree of avocado. The electrical impedance parameter especially impedance absolute magnitude is found to be most sensitive to ripening progression on avocado. In addition, the hypothesis of distinguishing ripening states based on EIS is confirmed by principal component analysis over frequency dependent electrical response. A classifier, based on multiclass Support Vector machines, is designed and it shows excellent discriminant capabilities of EIS technique to track and analyze 4 ripening stages (firm, breaking, ripe and overripe) of avocado.

Assessment of Ripening Degree of Avocado by Electrical Impedance Spectroscopy and Support Vector Machine

Monzurul Islam[1], Khan Wahid[1], Anh Dinh[1]

[1] Department of Electrical and Computer Engineering, University of Saskatchewan, Saskatoon S7N 5A2, Canada.

Correspondence should be addressed to Monzurul Islam; moi352@mail.usask.ca

Abstract

Avocado, a climacteric fruit, exerts high rate of respiration and ethylene production and thereby subject to ripening during storage. Therefore, its ripening is a significant factor to impart optimum quality in post-harvest storage. To understand the dynamics of ripening and to assess the degree of ripening in avocado, electrical sensing technique is utilized in this study. In particular, Electrical Impedance Spectroscopy (EIS) is found to uncover the physiological and structural characteristics in plants and vegetables and to follow physiological progressions due to environmental impacts. In this work, we present an approach that will integrate EIS and machine learning technique that allows us to monitor ripening degree of avocado. It is evident from our study that the impedance absolute magnitude of avocado gradually decrease as the ripening stages (firm, breaking, ripe and overripe) proceed at a particular frequency. In addition, Principal component analysis shows that impedance magnitude (two principal components combined explain 99.95 % variation) has better discrimination capabilities for ripening degrees compared to impedance phase angle, impedance real part and impedance imaginary part. Our classifier utilizes two principal component features over 100 EIS responses and demonstrate classification over firm, breaking, ripe and overripe stages with an accuracy of 90%, precision of 93%, recall of 90%, f1-score of 90% and auc of 88%. The study offers plant scientists a low cost and nondestructive approach to monitor post-harvest ripening process for quality control during storage.

4.1 Introduction

Avocados receive an increasing attention for extending nutritional food choice and agribusiness in United States [1]. According to a recent report from National Agricultural Statistics

Service of United States Department of Agriculture, the value of U.S. avocado production measured $316 million in 2016-17 [2] and U.S. consumption of avocados increased significantly from 1.1 pounds per capita in 1989 to a record 7.1 pounds per capita in 2016. Avocado, being a climacteric fruit, has a high rate of post-harvest respiration. Consequently, it is one of the most perishable fruits and has very limited shelf life. It is prone to biochemical and physiological deterioration during post-harvest ripening accompanied by degradation of visual appearance. This post-harvest loss poses the risk of loss of market value of avocado. In addition, from the point of view of consumer industry, only optimum ripening state attributes to the most nutritional value and best taste of a fruit. Hence, a better understanding of ripening dynamics of avocado can play a vital role to the development of appropriate tool for better packaging, storage and transportation process and consequently meet the demand of both agribusiness and consumer industry.

Conventional chemical and biochemical analyses conducted to investigate the fruit ripening are limited by factors like processing time and destructive nature [3]. These methods are often laborious, expensive and requires access to laboratory facility. Hence, these methods proves to be infeasible for a repetitive inspection. Therefore, it is essential to expand current technologies from different viewpoints. A nondestructive, low cost and easily accessible solution to this issue needs to be devised.

Nondestructive methods like Magnetic Resonance Imaging (MRI) and CT Scan are found to be effective towards understanding of ripening, internal fruit quality and postharvest processing [4, 5]. MRI method requires separation of signal of water proton from that of fat proton which is still a challenging task. And both MRI and CT are limited by the factors such as high cost and processing complexity. Hyperspectral imaging can effectively assess ripening degrees [6] but it also suffers from constrains like cost and processing. Therefore, it is essential to expand current technologies from different viewpoints. On the contrary, Electrical Impedance Spectroscopy (EIS) is a fast, low cost and nondestructive method which is found to offer insight into plant physiology and physiological dynamics due to environmental impacts. In this direction, the EIS studies have been conducted as a nondestructive evaluation method to the investigate impedance spectrum variations and to determine the ripening degree in avocado.

To develop an easily accessible and non-destructive method to understand mechanisms of ripening and to assess ripening degree of avocado, the prospect of EIS technique is explored in

this paper. This work on avocado mainly focuses on the investigation of feasibility of EIS for assessment of ripening degree nondestructively. The rest of the paper is organized as follows: related past works on application of EIS technique is reviewed in Literature Review section. Next Section introduces the theory of bio-impedance and Electrical Impedance Spectroscopy. Later on, experimental methods and materials are illustrated. After that the experimental and simulated results are presented and discussed and finally paper is concluded including some future exploration directions.

4.2 Literature Review

Impedance sensing technology especially EIS has emerged a new era into food quality and stability over the last decades. It has been extensively used in the field of plant physiology, agriculture and food engineering for quality control and assessment of fruits and vegetables such as Banana [7], Garut citrus [8] , kiwi [9], Lettuce [10], Nectarine [11], Strawberry [12]. In order to assess the freshness of banana, EIS investigation was performed during different ripening state [7]**.** By attaching Ag/AgCl electrode and injecting a small amount of current, impedance responses are measured by the 4294A Impedance Analyzer over a frequency range of 50Hz to 1MHz. The impedance magnitude, phase angle, real and imaginary part varied markedly with the alteration of ripening state.

Authors in [13] designed a nondestructive device to obtain the impedance spectrum of the whole strawberry fruit and later on performed classification by utilizing corresponding equivalent circuit parameters (Constant Phase Element, CPE-P and $R_{infinity}$). The study showed that the strawberries at the highest stage of ripeness had significantly lower constant phase element and Ro (related to extra-cellular) values compared to other strawberries.

Neto, et al. [14] utilized EIS technique for the determination of the maturation degree of mangoes based on variation of bulk resistance dependence with maturation of fruits. They came up with this strategy to normalize bulk resistance by diameter to compensate the size variations of samples. They demonstrated good agreement between variation of electrical response and mechanical response of fruit.

Montoya, et al. [15] investigated that electrical conductivity could be a suitable factor for assessment of quality during ripening and cold storage. The found some resemblance between electrical conductivity response and ethylene productions curve. They defined a threshold of conductivity (0.24 S/m) that indicates the limiting value for fruit stored at non-injurious temperatures and subsequently transferred to 20°C for marketing.

Chowdhury, et al. [16] carried out EIS study on mandarin orange fruit during ripening in a spectrum between 50 Hz to 1 MHz. They observed significant variation of the impedance, phase angle, real and imaginary part of the impedance with different state of orange ripening. The study also demonstrated loss of weight of corresponding samples with the progression of ripening states. Thus, electrical sensing specially EIS technique was found to offer insight into physiology of fruits and vegetables undergoing the ripening process.

4.3 Materials and methods

4.3.1 EIS Measurement

Impedance measurement on avocado was carried out with the EVAL-AD5933 Evaluation Board, a high precision impedance converter system. The device integrates an on-board frequency generator, a 12-bit 1 MSPS analog-to-digital converter (ADC), and an internal temperature sensor. Both the excitation signal and response signal are sampled by ADC and Fourier transformed by on-board DSP engine in order to obtain complex impedance spectrum. The frequency range of AD5933 is from 5 kHz up to 100 kHz without external components and lower frequencies than 5 KHz are achievable using an external divider. The device has a master clock of 16.77 MHz and supply voltage requirement of 2.7 V to 5.5 V. The device comes in a 16-SSOP package that has a temperature range of -40°C to +125°C. The device offers high accuracy and versatility that make it suitable for electrochemical analysis, corrosion monitoring, automotive sensors, proximity sensing and bio-impedance measurements.

The experimental setup of EIS data acquisition system is presented in Figure 4.1a. The graphical user interface of the supporting software is presented in Figure 4.1b. The electrode holder platform has a height of 10 centimeter and the holder is horizontally movable and vertically rotatable. A noninvasive two-electrode measurement system was employed in our experiment where ‘alligator’ type Ag electrode clips were connected with circular electrode plates from ECG

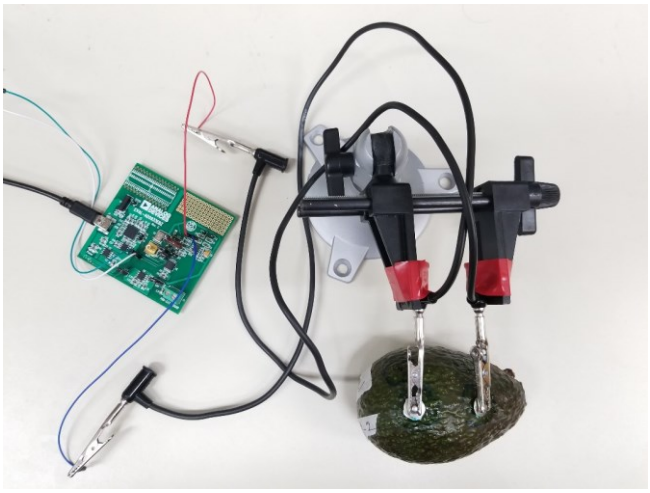

(a)

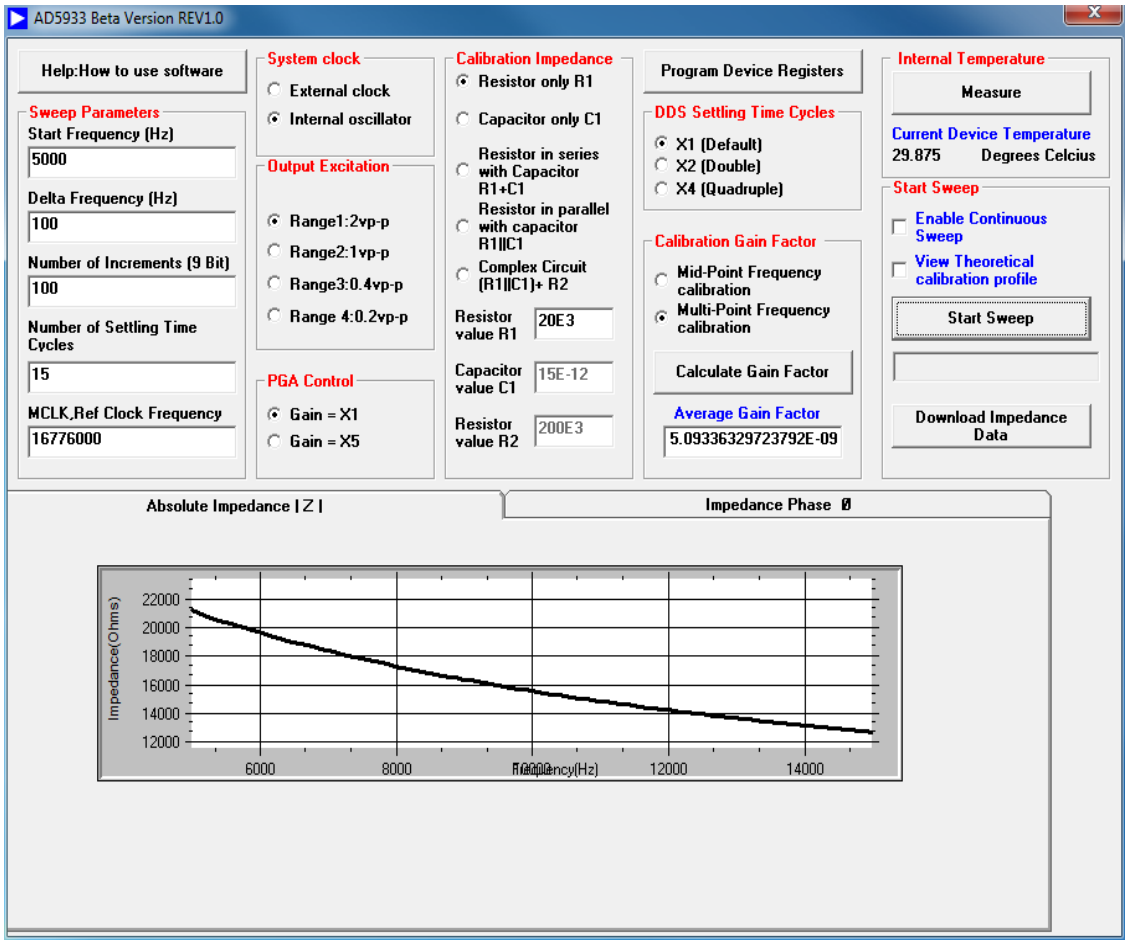

(b)

Figure 4.1: Hardware and software utilized for data acquisition: (a) AD5933 evaluation board and (b) snapshot of the supporting software's graphic user interface.

electrode and finally ‘alligator’ clips were tied with the electrode holders. Similar separations of 4.4 centimeter between two electrodes were maintained for all measurement. To compensate the contact resistance, a layer of electrode gel (‘Spectra 360’ salt-free electrode gel) was placed between ECG electrode plate and test subject (avocado fruits). For impedance spectroscopy measurements in this study, we used a 1V p-p generator voltage and scanned 101 spot frequencies (frequency intervals) between 5 KHz to 15 KHz. The AC signal injected into the sample was generated by the built-in function generator of the evaluation board.

The avocado fruits for our experiment were collected from a local supermarket. During the period of experiment, avocados were kept in the lab environment. The temperature in the lab was 20 degree Celsius and relative humidity was 40%. Further experiment can be conducted with freshly harvested avocados and stored in different controlled temperatures in future studies.

4.3.2 Feature Extraction by Principal Component Analysis

Principal Component Analysis (PCA) is mathematically defined as an orthogonal linear transformation that converts a set of data (possibly correlated) into a new set of linearly uncorrelated data called principal components. The first principal component contains the largest percentage of data variance and the variance decreases in the following principal components. In this study, PCAs were carried out with data obtained from the samples in order to assess the feasibility of the EIS technique to discriminate among different ripening stages of avocado. PCA served the purpose of dimensionality reduction and feature extraction on EIS data. PCA was performed over impedance magnitude, impedance phase angle, impedance real part and impedance imaginary part over the predefined frequency range where the device shows maximum sensitivity.

4.3.3 Classification by Multiclass Support Vector Machine (SVM)

Support Vector Machines (SVMs) are supervised learning models which construct an optimal hyperplane to classify data into different classes. And lines drawn parallel to this separating line are the supporting hyperplanes and the distance between them is called the decision margin. Width of the margin is constrained by support vectors which are the data points that are

closest to the separating hyperplane. Since, the optimal hyperplane is the one that separates the high probability density areas of the classes with maximum possible margin between them, the goal is to determine the direction that provides the maximum margin. It needs the solution of following optimization problem in Equation (4.1) for a given training set of instance label pairs (x_l, y_l), $l = 1, 2, ..., i$ where $x_l \in R^n$ and $y_l \in \{1, -1\}^i$.

$$\min_{u,e,\xi} \frac{1}{2} u^T u + C \sum_{l=1}^{i} \xi_l \tag{4.1}$$

$$\text{subjected to } y_l = (u^T \phi(x_l) + e) \geq 1 - \xi_l \quad , \xi_l \geq 0 .$$

For quantitate analysis of discrimination of ripening degrees based on EIS data, a multiclass support vector machine was modeled. The ground truths for all the samples were generated by subjective testing. In this direction, ripening chart and ripening information of avocado were utilized. The ripening chart of avocado used in this experiment is presented in Figure 4.2.

Figure 4.2 Ripening chart of Avocado [18]

4.4 Result and Discussion

Ripening is the process by which fruits attain their desirable color, flavor, palatable nature and other textural properties that make the fruit acceptable for consumption. Ripening is associated with change in biochemical composition that is conversion of starch to sugar. Avocado, being a

climacteric fruit, continue to ripen after harvest. During the ripening process, it emits ethylene along with increased rate of respiration.

The EIS study on avocado was undertaken with an attempt to better understand and identify the ripening stages of avocado in term of electrical Bio-impedance. The EIS studies conducted for avocado sample show that at a particular frequency (especially for less than 10 KHz), the avocado impedance magnitude gradually decreases as ripening stages (firm, breaking, ripe and overripe) proceed (Figure 4.3a). And for a particular maturity degree, impedance magnitude decreased significantly from low to high frequency especially for firm, breaking and ripe stages. At lower frequency, the electrical current flows only through extracellular fluids which acts as electrolytes and have relatively high resistance. The cell membrane exert extreme high capacitance at low frequency and that's why electrical current can't pass through intracellular fluid and only flows through the extracellular fluid. At high frequency, cell membrane capacitance reduces significantly and current flows through intracellular fluid, which has relatively low resistance. This is how impedance decline markedly from low to high frequency area of impedance spectra. This phenomenon resulting from cell structures in biological tissue is known as β dispersion. Figure 4.3b shows that the phase angle of avocado impedance varies with frequency throughout the ripening stages. At a particular frequency, the avocado impedance phase angle gradually increases

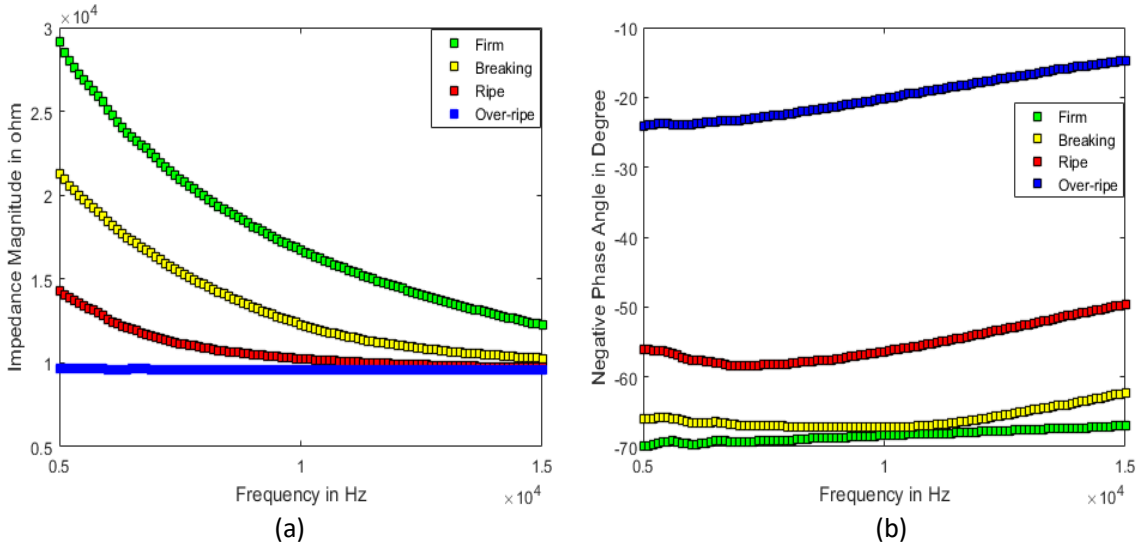

Figure 4.3 EIS response of Avocado during ripening: (a) Impedance Magnitude vs. Frequency (b) Negative Phase Angle vs. Frequency

as ripening stages (firm, breaking, ripe and overripe) proceed (Figure 4.3b). And especially on high frequency range of the spectrum (10 KHz to 15 KHz), for a particular maturity degree, impedance phase angle rises as the frequency increases.

EIS study on avocado was extended to multiple samples to uncover the dynamics of

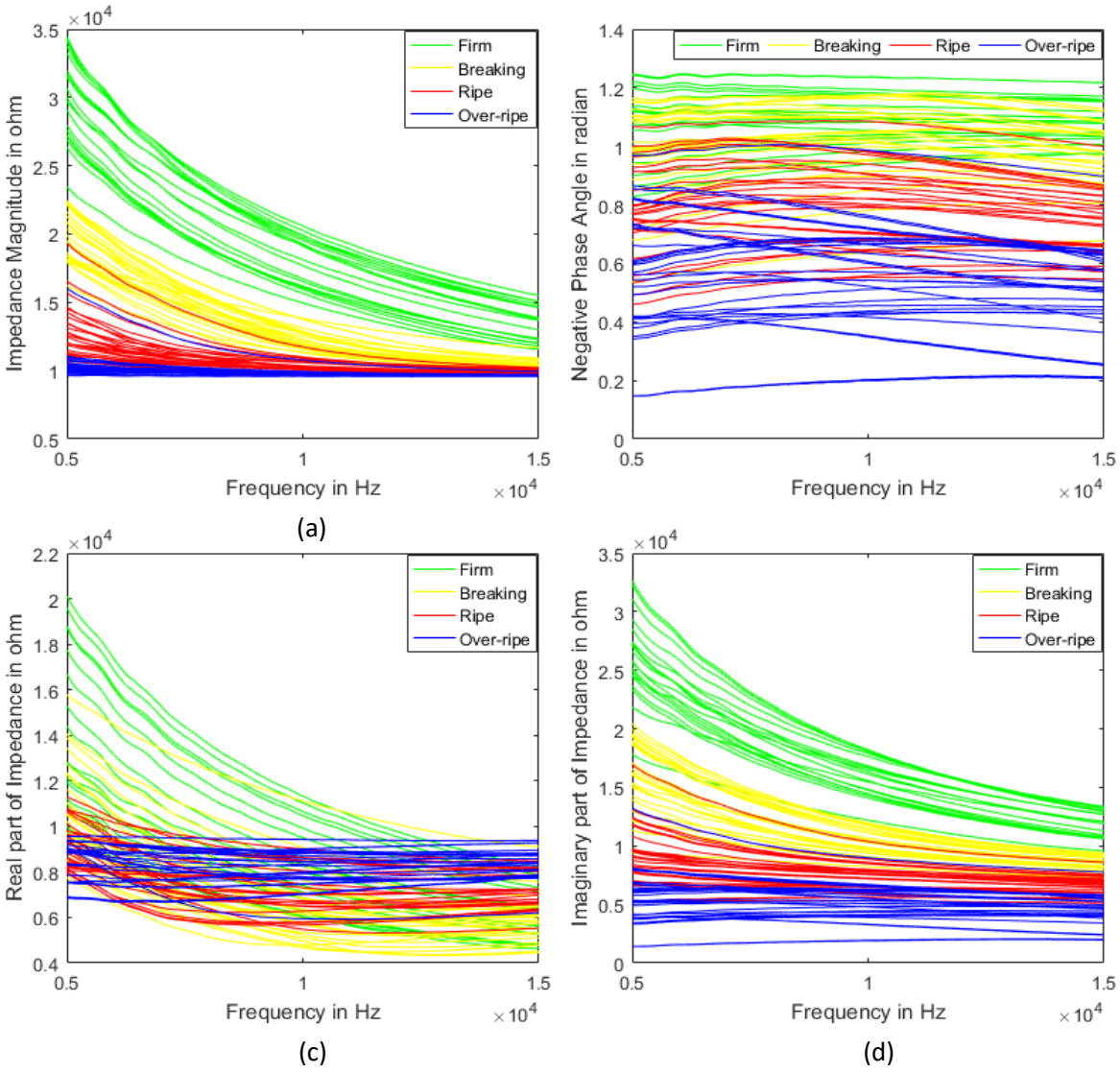

Figure 4.4 EIS response of all experimental Avocado samples during ripening: (a) Impedance Magnitude vs. Frequency (b) Negative Phase Angle vs. Frequency (c) Real part of impedance vs. Frequency and (d) Imaginary part of Impedance vs. Frequency

ripening with respect to impedance-frequency response. One hundred different EIS responses belonging to different ripening degrees were recorded and presented in Figure 4.4. It can be intuitively concluded that impedance magnitude best reflects the ripening degrees.

Now to better visualize and analyze the large data obtained from all EIS responses, principal component analysis (PCA) was carried out over impedance magnitude, impedance phase angle, impedance real part and impedance imaginary part. Furthermore, PCA was used to obtain a reduced number of uncorrelated variables, which are the principal components (PCs). PCA was able to reduce the initial 101 variables (for every impedance parameter) to 2 PCs which combined explained a significant percentage of the total variance. The first principal component and second

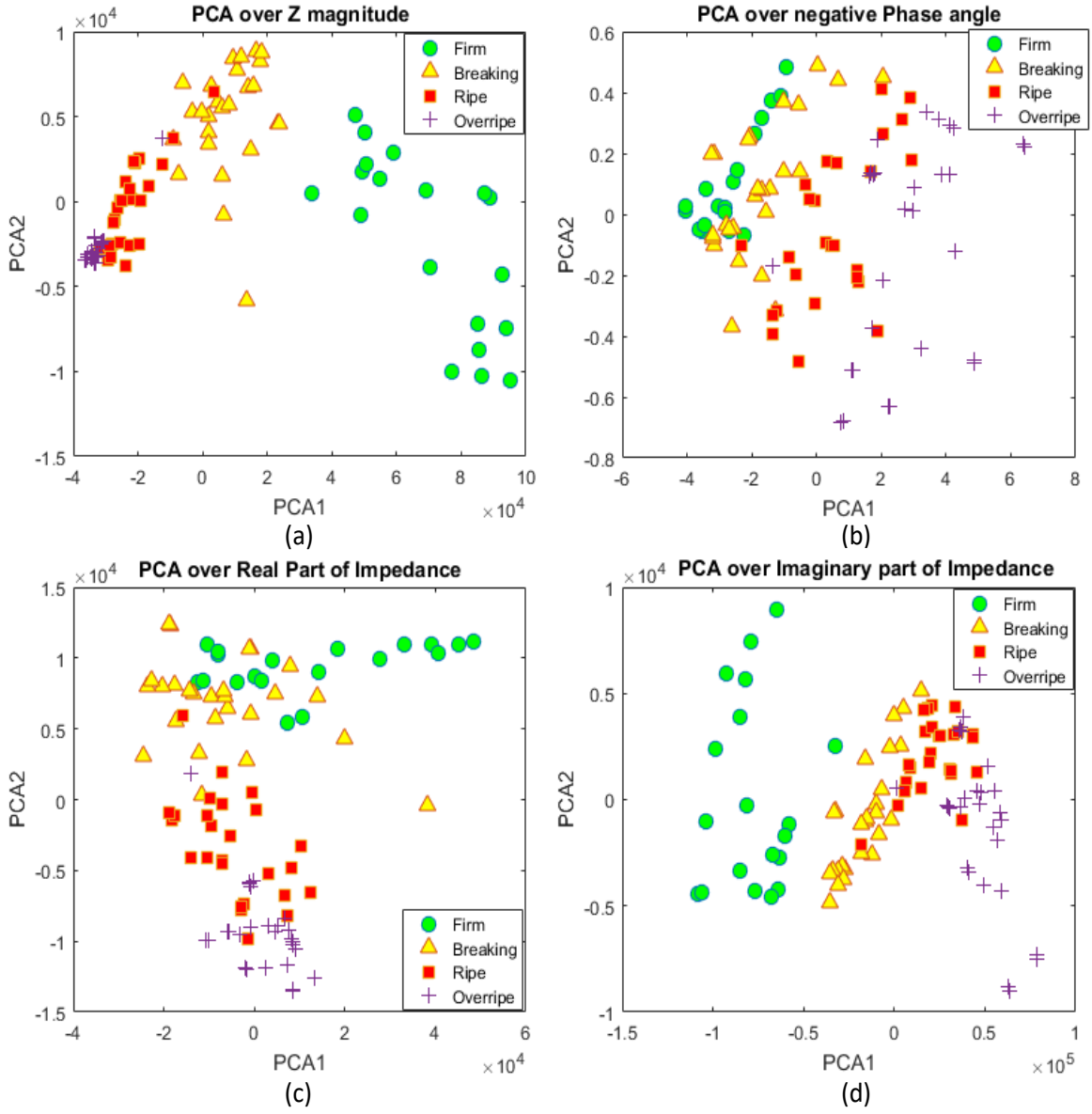

Figure 4.5 Principal Component Analysis (PCA2 Vs. PCA1) over EIS responses: (a) Impedance Magnitude (b) Negative Phase Angle (c) Real part of impedance and (d) Imaginary part of Impedance.

principal component over Impedance magnitude explained respectively 98.67% and 1.28% of total variance in the data. PCA over impedance magnitude, impedance phase angle, impedance real part and impedance imaginary part are demonstrated respectively in Figure 4.5a, 4.5b, 4.5c and 4.5d. Especially in the PCA2–PCA1 score plot of Impedance Magnitude (Figure 4.5a), it is apparent that the data for every ripening degrees tend to cluster and in general and four different zone can be separated. It is evident that PCA feature from impedance magnitude has better discrimination capabilities for ripening degrees compared to impedance phase angle and impedance real part and impedance imaginary part.

In addition, for quantitate investigation of the prospect of EIS parameters towards discrimination of ripening degrees; a supervised classifier model was developed. Our experimental dataset is composed of 100 EIS responses containing 19 responses from firm class, 26 from breaking class, 26 from ripe class and 29 from overripe class. During experiment, the database was divided into two sets: the training set containing 60 responses and the testing set containing 40 responses. For feature extraction from EIS data, PCA was carried out over impedance magnitude, impedance phase angle, impedance real part and impedance imaginary part. Analyzing discrimination capabilities of different Impedance parameters, only PCA1 and PCA2 over impedance magnitude were selected to feed to our classifier. For classification purpose, a multiclass support vector machine with 'linear' Kernel was utilized. For performance evaluation of the classification model, performance parameters such as accuracy, precision, recall, and F1-score were calculated. Accuracy, most intuitive performance measure, is simply a ratio of correctly predicted observation to the total observations. Precision is the ratio of correctly predicted positive observations to the total predicted positive observations. The recall is intuitively the ability of the classifier to find all the positive samples. The F-beta score can be interpreted as a weighted harmonic mean of the precision and recall. At the 60%-40% train-test split, testing accuracy of the classification was 90%. The other performance measures are illustrated in Table 4.1.

To assess the accuracy of a classification, it is common practice to create a confusion matrix where classification results are compared to additional ground truth information. Figure 4.6 shows the graphical representation of the confusion matrix containing test data for firm (class 0), breaking (class 1), ripe (class 2) and overripe (class 3).

A receiver operating characteristic (ROC) curve is created by plotting the true positive rate (TPR) against the false positive rate (FPR) at various threshold settings. It illustrates the diagnostic ability of a classifier system and the area under ROC curve, called AUC, is an effective summarize of its performance. Figure 4.7 shows that the average area under the ROC curve is 88% that indicates excellent discrimination capabilities of our classifier.

Table 4.1 Performance Scores of proposed algorithm

Class	Performance Scores		
	Precision	Recall	F1-score
0: Firm	1.00	1.00	1.00
1: Breaking	1.00	0.80	0.89
2: Ripe	0.71	1.00	0.83
3: Overripe	1.00	0.83	0.91
Average / Total	0.93	0.90	0.90

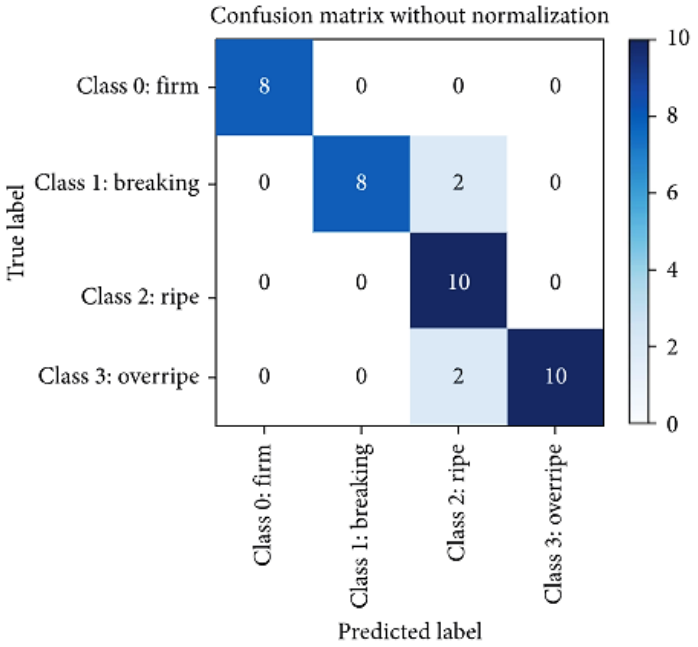

Figure 4.6 Plot of Confusion Matrix for test data

In 2011, a study was performed by authors [17] to investigate the ripening process of mango utilizing Electrical Impedance Spectroscopy technique. To discriminate raw and ripe mango fruits, they measured bulk impedance by LCR meter and expressed in terms of effective resistance and effective capacitance in the frequency range of 1 to 200 KHz. They came up with a ratio of effective resistance of ripe to raw fruit that is significant enough at 1 KHz to characterize raw and ripe state. They also found the ratio of effective capacitance of raw and ripe mango and concluded that the ratio of effective resistance show better discrimination capabilities at 1-6 KHz compared to effective capacitance. In our study, we differentiated among four ripening states of

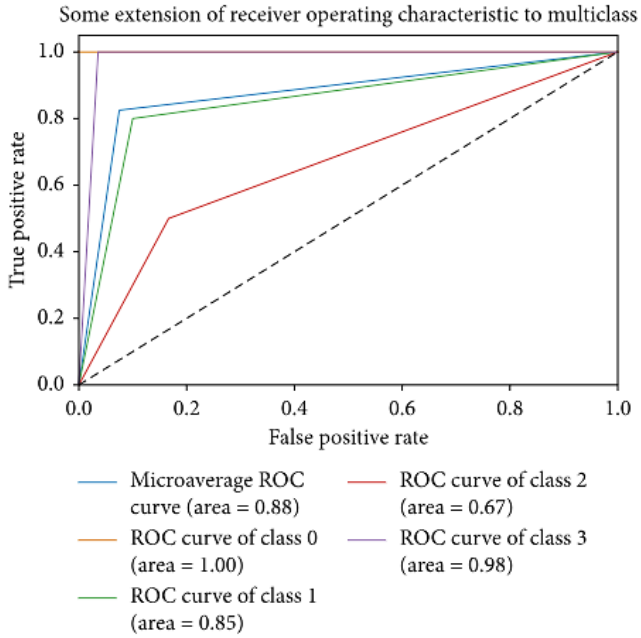

Figure 4.7 ROC analysis of ripening stage classification

avocado utilizing impedance spectra at 5 KHz to 15 KHz utilizing Ad5933 evaluation board. This impedance converter board is low cost compared to the LCR-800 GW Instek in their study. Also it supports automated frequency sweep which their LCR meter lacks. The feature extraction by principal component analysis over Impedance magnitude directly (instead of effective resistance or capacitance) was enough for our support vector machine classifier. Whereas their study only differentiated binary classes (raw and ripe), we performed multiclass classification among firm, breaking, ripe and overripe avocado. The study offers plant scientists a low cost and nondestructive approach to monitor post-harvest ripening process of avocado for quality control during storage.

4.5 Conclusion

The feasibility of electrical impedance spectroscopy, a nondestructive technique, to assess the ripening degree of avocado has been explored in this study. A low cost, easily accessible and nondestructive system based on ad5933 impedance analyzer has been investigated in this work. The electrical impedance parameter especially impedance absolute magnitude is found to be most sensitive to ripening progression on avocado. In addition, principal component analysis over frequency dependent electrical response corroborates the hypothesis of distinguishing ripening states based on EIS. Our classifier based on multiclass Support Vector machines shows excellent discriminant capabilities of EIS technique to track and analyze 4 ripening stages (firm, breaking, ripe and overripe) of avocado. This approach can be a potential alternative to conventional chemical analysis techniques with offering of better time and cost saving and less processing complexity. Proposed system can be extended and tested to other fruits for analyzing their ripening dynamics nondestructively and to be addressed in future studies.

Conflicts of Interest

The authors declare that there is no conflict of interest regarding the publication of this paper.

References

[1] M. Wien, E. Haddad, K. Oda, and J. Sabaté, "A randomized 3x3 crossover study to evaluate the effect of Hass avocado intake on post-ingestive satiety, glucose and insulin levels, and subsequent energy intake in overweight adults," *Nutrition journal,* vol. 12, p. 155, 2013.

[2] National Agricultural Statistics Service: United States Department of Agriculture, "Noncitrus Fruits and Nuts 2016 Summary," June 2017. Available: https://www.nass.usda.gov/Publications/Todays_Reports/reports/ncit0617.pdf.[Accessed: Dec. 17, 2018].

[3] K. Miloski, K. Wallace, A. Fenger, E. Schneider, and K. Bendinskas, "Comparison of biochemical and chemical digestion and detection methods for carbohydrates," *American Journal of Undergraduate Research,* vol. 7, pp. 48-52, 2008.

[4] M. K. Abera, S. W. Fanta, P. Verboven, Q. T. Ho, J. Carmeliet, and B. M. Nicolai, "Virtual fruit tissue generation based on cell growth modelling," *Food and Bioprocess Technology,* vol. 6, pp. 859-869, 2013.

[5] L. Zhang and M. J. McCarthy, "Measurement and evaluation of tomato maturity using magnetic resonance imaging," *Postharvest Biology and Technology,* vol. 67, pp. 37-43, 2012.

[6] R. Khodabakhshian and B. Emadi, "Application of Vis/SNIR hyperspectral imaging in ripeness classification of pear," *International Journal of Food Properties,* vol. 20, pp. S3149-S3163, 2017.

[7] A. Chowdhury, T. Bera, D. Ghoshal, and B. Chakraborty, "Studying the electrical impedance variations in banana ripening using electrical impedance spectroscopy (EIS)," in *Computer, Communication, Control and Information Technology (C3IT), 2015 Third International Conference on*, 2015, pp. 1-4.

[8] J. Juansah, I. W. Budiastra, K. Dahlan, and K. B. Seminar, "The prospect of electrical impedance spectroscopy as non-destructive evaluation of citrus fruits acidity," *Int. J. Emerg. Technol. Adv. Eng,* vol. 2, pp. 58-64, 2012.

[9] Y. Tang, G. Du, and J. Zhang, "Change of electric parameters and physiological parameters of kiwi of storage period," *Nongye Jixie Xuebao(Transactions of the Chinese Society of Agricultural Machinery),* vol. 43, pp. 127-133, 2012.

[10] R. F. Muñoz-Huerta, A. d. J. Ortiz-Melendez, R. G. Guevara-Gonzalez, I. Torres-Pacheco, G. Herrera-Ruiz, L. M. Contreras-Medina*, et al.*, "An analysis of electrical impedance measurements applied for plant N status estimation in lettuce (Lactuca sativa)," *Sensors,* vol. 14, pp. 11492-11503, 2014.

[11] M. D. O'Toole, L. A. Marsh, J. L. Davidson, Y. M. Tan, D. W. Armitage, and A. J. Peyton, "Non-contact multi-frequency magnetic induction spectroscopy system for industrial-scale bio-impedance measurement," *Measurement Science and Technology,* vol. 26, p. 035102, 2015.

[12] J. R. GONZÁLEZ ARAIZA, "Impedancia Bio-Electrica Como Técnica No-Destructiva para Medir la Firmeza de la Fresa (Fragaria x Ananassa Duch) y su Relación Con Técnicas Convencionales," 2014.

[13] J. R. González-Araiza, M. C. Ortiz-Sánchez, F. M. Vargas-Luna, and J. M. Cabrera-Sixto, "Application of electrical bio-impedance for the evaluation of strawberry ripeness," *International Journal of Food Properties,* vol. 20, pp. 1044-1050, 2017.

[14] A. F. Neto, N. C. Olivier, E. R. Cordeiro, and H. P. de Oliveira, "Determination of mango ripening degree by electrical impedance spectroscopy," *Computers and Electronics in Agriculture,* vol. 143, pp. 222-226, 2017.

[15] M. Montoya, J. De La Plaza, and V. López-Rodriguez, "Electrical conductivity of avocado fruits during cold storage and ripening," *LWT-Food Science and Technology,* vol. 27, pp. 34-38, 1994.

[16] A. Chowdhury, P. Singh, T. K. Bera, D. Ghoshal, and B. Chakraborty, "Electrical impedance spectroscopic study of mandarin orange during ripening," *Journal of Food Measurement and Characterization,* vol. 11, pp. 1654-1664, 2017.

[17] M. Rehman, B. A. Abu Izneid, M. Z. Abdullah, and M. R. Arshad, "Assessment of quality of fruits using impedance spectroscopy," *International journal of food science & technology,* vol. 46, pp. 1303-1309, 2011.

[18] Love One Today, "How to Pick & Buy Fresh Avocados," [online]. Available: https://loveonetoday.com/how-to/pick-buy-fresh-avocados/. [Accessed: Dec. 17, 2018].

Chapter 5 – Design of a low Cost EIT System and Application on Root Imaging

Manuscript prepared as M. Islam, K. Wahid and A. Dinh, "Design of a low cost EIT system and application on root imaging," *to submit to Sensors*. The manuscript is modified and reorganized according to the writing style of this thesis. The manuscript is written by me (M. Islam) under the supervision of K. Wahid and A. Dinh. Reviewing the literature, designing and performing the experiment and analysis of result were done by me (M. Islam) under the supervision of K. Wahid and A. Dinh.

The chapter presents the development of a low cost, low power, semi-automated, lightweight and small form factor electrical impedance tomography data acquisition system. The system is capable of performing both single and multi-frequency EIT in both 2D and 3D domain. It also offers the ability of imaging living and nonliving subject. The reconstructed results allows to determine the size, shape, and location of the subject under test. The prospect of the system for nondestructive modeling of plant root in hydroponics is also explored. The system able to image weed and carrot roots in 3D in the water medium. Furthermore, the prospect of determining root biomass using raw EIT data is also explored in this chapter.

Design of a Low Cost Electrical Impedance Tomography System for Modeling of Root

Monzurul Islam[1], Khan Wahid[1], Anh Dinh[1]

[1]*Department of Electrical and Computer Engineering, University of Saskatchewan, Saskatoon, SK, Canada*

Contact email: moi352@mail.usask.ca

Abstract

An insight into plant's health especially root system can impart better crop performance and eventually ensure food sustainability. In this study, we present a low cost root imaging device based on Electrical Impedance Tomography. Electrical Impedance Tomography (EIT) is a noninvasive and nondestructive imaging technique that exploits the electrical conductivity, permittivity and impedance change by the array of electrodes around the test subject. Firstly, a small alternating current is applied, the resulting potentials are recorded from the other electrodes and repeating the process for all possible electrode-pair combination, a final tomographic image is reconstructed. Hence, this work designed, developed and implemented a low cost EIT system and analyzed root imaging as well. The prototype contains an electrode array system, an impedance analyzer board, 2 multiplexer units, and an Arduino. The Eval-Ad5933-EBZ, a high precision impedance converter and network analyzer system, is used for measuring the bioimpedance of the root. The electrode array contains 8 electrodes in every layer surrounding the test subject. Two CD74HC4067 16-to-1 multiplexers are used as electrode switching unit to select all injection-sense electrode pairs, and both multiplexers and controlled by an Arduino. By performing Finite Element Analysis and solving forward and inverse problems, the tomographic image of the root is reconstructed. The system was able to localize and build 2D and 3D tomographic image of the root in a liquid medium. This low-cost and easy-to-access system enables us to capture repetitive, noninvasive and nondestructive image of living plant roots. Furthermore, a simple mathematical model was proposed, based on ridge regression, to predict root biomass from EIT data nondestructively with an accuracy of more than 93%. Thus, the device offers plant scientists and crop consultants the ability to better understand root system without harming the plant.

5.1 Introduction

Electrical Impedance Tomography (EIT) [1-3] is a noninvasive imaging technique where the electrical conductivity, permittivity, and impedance of an object is measured by an array of electrodes around it and by utilizing the measured data at domain boundary, a tomographic image of the object is reconstructed. In EIT, a constant current signal is injected into the object and the boundary potentials data are measured through the surface electrodes using an EIT instrumentation [4-6]. Using the boundary voltage-current data for solving an inverse problem, a conductivity or resistivity distribution of the domain is obtained and thus EIT reconstruction is performed [7].

EIT is a fast, low cost, noninvasive, non-ionizing, radiation-free and portable imaging modality. Due to its unique advantages, EIT has obtained enormous attention and interest in diversified fields such as medical imaging, material engineering, Nanotechnology and MEMS , civil engineering, chemical engineering, biotechnology, and other fields of engineering, technology and applied sciences [8, 9]. In medical imaging, EIT has been extensively used for imaging of the lung [10, 11], studying the regional ventilation distribution in neonatal and pediatric lung disease [12], imaging of the breast [13] and brain [9]. EIT has been utilized in material engineering and the manufacturing technology such as studying the semiconductor manufacturing and estimating conductivity distribution of polysilicon thin film [14]. In nanotechnology, EIT has been studied for imaging of Carbon Nanotube (CNT) composite thin films [15, 16]. In several civil engineering applications and a number of research works on EIT have been reported such as imaging leaks from buried pipes [17] and brick walls imaging [18]. In biotechnology, EIT has been studied by several research groups for cell culture imaging by such as [19, 20].

Although not much works are found in the literature on the application of EIT on plant root, Weigand and Kemna [21] conducted a study on structural and functional imaging of crop root by EIT. The authors designed and conducted a controlled experiment in which the root systems of oilseed plants were monitored in a 2-D, water-filled rhizotron container with an array of 38 electrodes. The EIT imaging revealed low-frequency polarization response which attributes to crop root since the polarization response of water medium is insignificant. Based on a pixel-based Debye decomposition analysis of the spectral imaging results, the authors found a mean relaxation time of the root system's polarization signature in a frequency of 15Hz. For functional imaging, they applied nutrition stress over 3 days period and observed a gradual decrease of

polarization response from the root system. Thus they investigated the capability of EIT for imaging of root physiological process (stress).

This work designs and develops a low-cost EIT system from readily available off-the-shelf equipment and tests the validity of the system for imaging of plant root in hydroponics. The rest of the paper is organized as follows. Experimental methods and materials are illustrated in section 5.2. The results are presented and discussed in Section 5.3. Finally, the study is concluded in section 5.4.

5.2 Materials and Methods

The EIT system consists of five main units: a multi-electrode sensor, a switching unit, a microcontroller, an impedance analyzer and a computer for reconstruction. Figure 5.1 shows the flowchart of the architecture of our EIT system. A high precision impedance analyzer Eval-AD5933 performs the measurement of complex electrical impedance. Between impedance analyzer and the electrode arrays, there are switching units for selecting the desired electrode patterns. A low-cost 16-to-1 multiplexer, CD74HC4067, is used as the switching unit. Both the switching units and the impedance analyzer are controlled by an Arduino. The Arduino automates the switching process by sending predefined 'switch select' signals to the multiplexers. Also, the initialization and calibration of the impedance converter board are performed by Arduino.

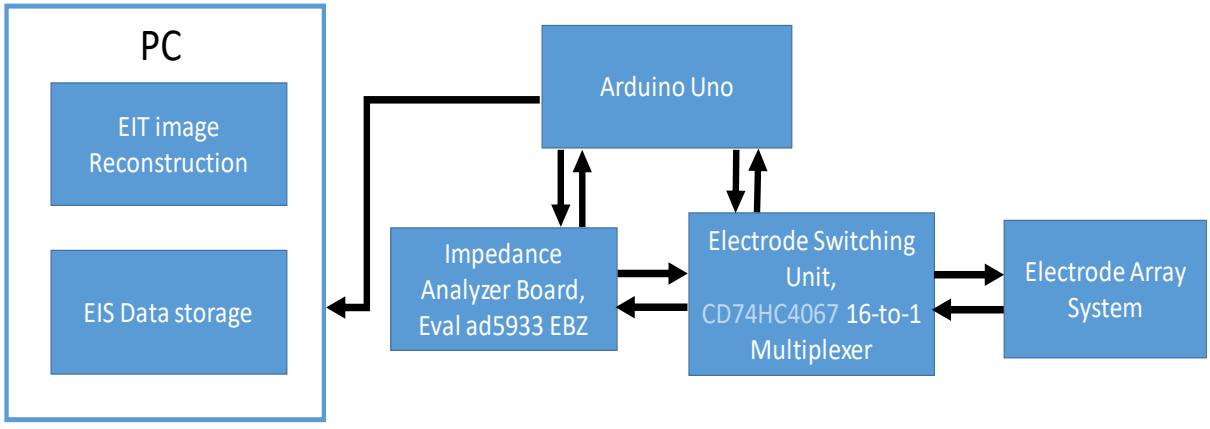

Figure 5.1: Architecture of our EIT system

Impedance measurement data from the Eval-AD5933 is transferred to Arduino by I2C protocol

and later on, the data are stored in the PC via serial COM ports. The prototype of the EIT data acquisition system is depicted in Figure 5. 2.

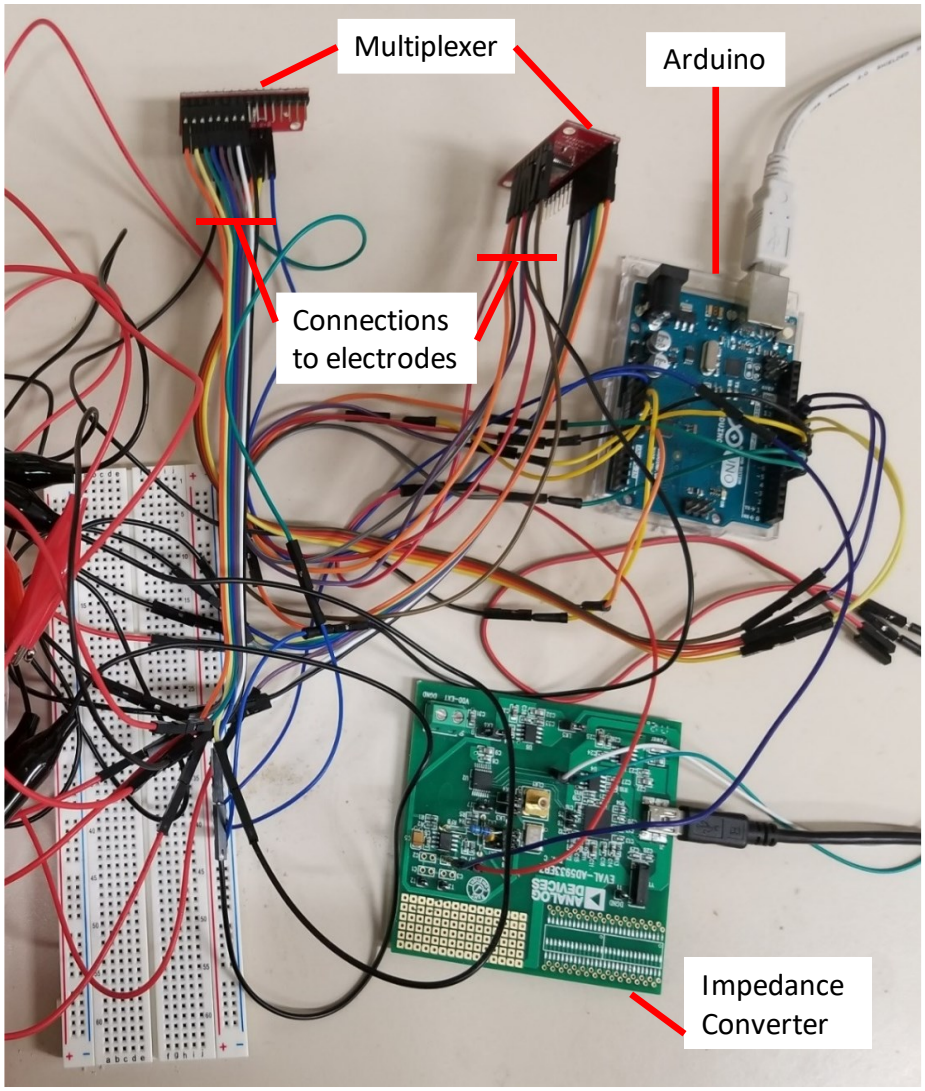

Figure 5.2 Prototype of our EIT data acquisition system

5.2.1 Eval AD5933 Impedance Converter

Impedance measurement is carried out with the EVAL-AD5933 Evaluation Board (Figure 5.3a), a high precision impedance converter system. The device integrates an on-board frequency generator, a 12-bit 1 MSPS analog-to-digital converter (ADC), and an internal temperature sensor.

Both the excitation signal and response signal are sampled by the ADC and Fourier transformed by the on-board DSP engine in order to obtain complex impedance spectrum. The frequency range of AD5933 is from 5KHz up to 100KHz without external components and frequencies lower than 5KHz are achievable using an external clock. The device has a master clock of 16.77MHz and supply voltage requirement of 2.7V to 5.5V. The device comes in a 16-SSOP package that has a temperature range of -40°C to +125°C. The device offers high accuracy and versatility that make it suitable for electrochemical analysis, corrosion monitoring, automotive sensors, proximity sensing, and bio-impedance measurements.

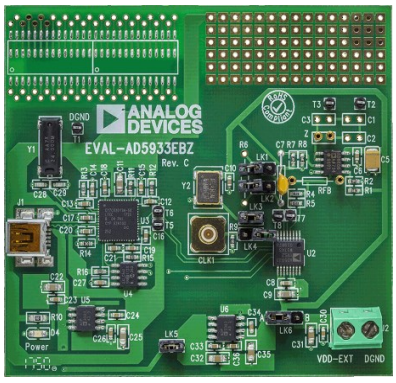

(a)

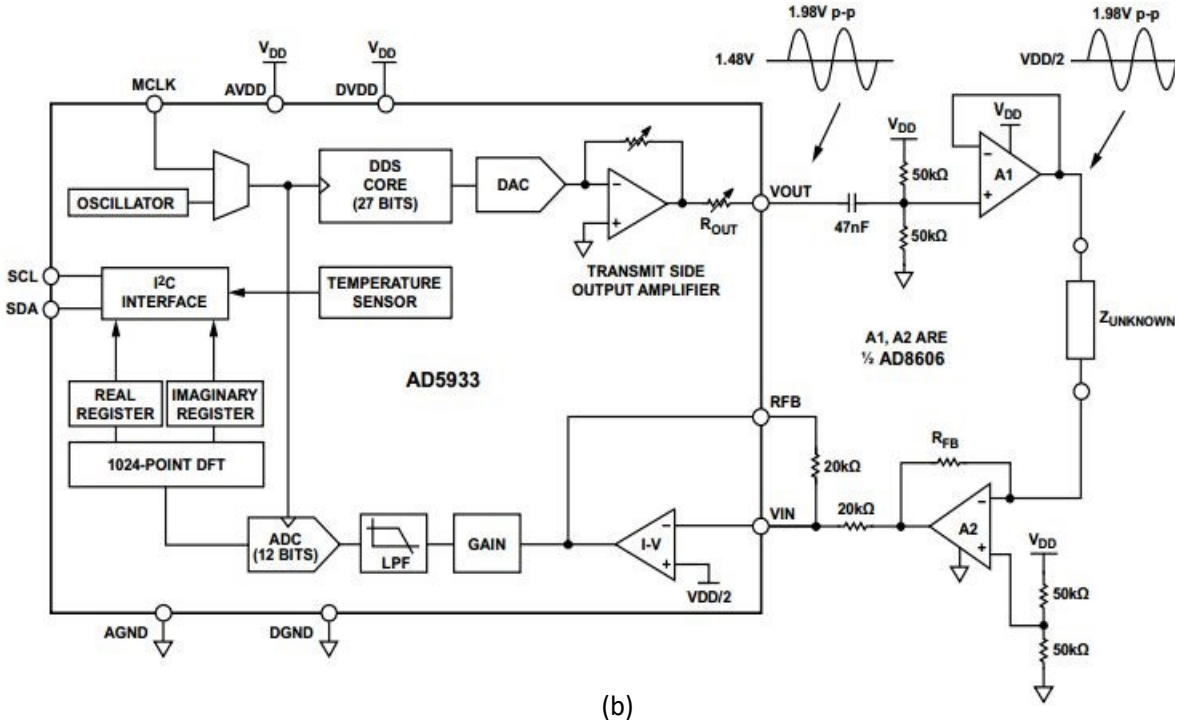

(b)

Figure 5.3 a) AD5933 evaluation board b) block diagram of the board

5.2.2 Analog Multiplexers

The CD74HC4067 chip based 16-Channel Analog Multiplexer (Figure 5.4) was used in the prototype. This multiplexer has 2V to 6V operational voltage and a wide operating temperature range of -55C to 125C. This CD74HC4067 chip acts as a rotary switch that routes the common pin to one of its 16 channel pins and vice versa. It works with both digital and analog signals (the voltage can't be higher than V_{CC}), and the connections function in either direction. By sending a binary sequence to the four switch select pins, 16 different pins can be routed to the signal pin. The internal switches are bidirectional, support voltages between ground and V_{CC}, have low "on" resistance and low "off" leakage, and to prevent crosstalk, perform "break-before-make" switching. The board also breaks out the chip's "enable" pin, which when driven high, will completely disconnect the common pin (all switches "off"). CD74HC4067 chip based 16-Channel analog multiplexer was used in the prototype to automate the electrode switching process.

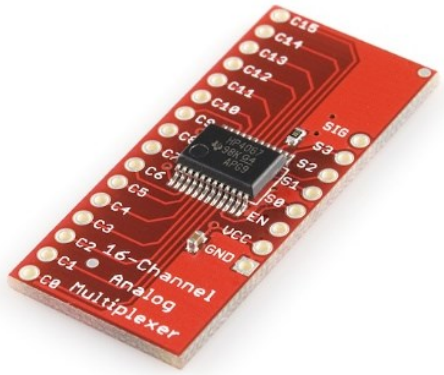

Figure 5.4 CD74HC4067 chip based 16-Channel Analog Multiplexer

5.2.3 Electrode Array System

Stainless steel paper clips are used as electrodes in our design. These electrodes are resistant to corrosion and unwanted chemical reactions. At the same time, they are extremely cheap and easy to install. A single layer of electrodes is used for 2D tomography and for 3D tomography, two or more layers are used. Every layer consists of 8 electrodes in our design (Figure 5.5). These paper clips are interfaced with the electrode switching unit via alligator clips and connecting wires.

5.2.4 Arduino Uno

Arduino Uno (Figure 5.6) is one of the most popular tools for rapid prototyping. Arduino Uno is a microcontroller board based on the ATmega328P. It has 14 digital input/output pins (of which 6 can be used as PWM outputs), 6 analog inputs, a 16 MHz quartz crystal, a USB connection, a power jack, an ICSP header, and a reset button. It has Flash Memory of 32 KB (ATmega328P) of which 0.5 KB used by bootloader. It has SRAM of 2 KB and EEPROM of 1 KB. It contains everything needed to support the microcontroller; the users need to simply connect it to a computer with a USB cable or power it with an AC-to-DC adapter or a battery to get started. Some I/O pins have alternative functionalities analog/digital I/O such as SPI, external interrupts, SCL and SDA. Thus Arduino supports SPI and I2C communication protocols.

In this work, Arduino Uno was used to control the impedance converter and the multiplexer switching units. Arduino Uno also perform the initialization and calibration of the impedance converter. Important setting-parameters of the converter such as frequency range for frequency-sweep, reference clock frequency, output excitation range are set by Arduino Uno. Besides, during electrode switching, Arduino Uno imposes time delay to ensure the stability of measurement. It also sends the measured impedance parameters to a PC via serial COM port.

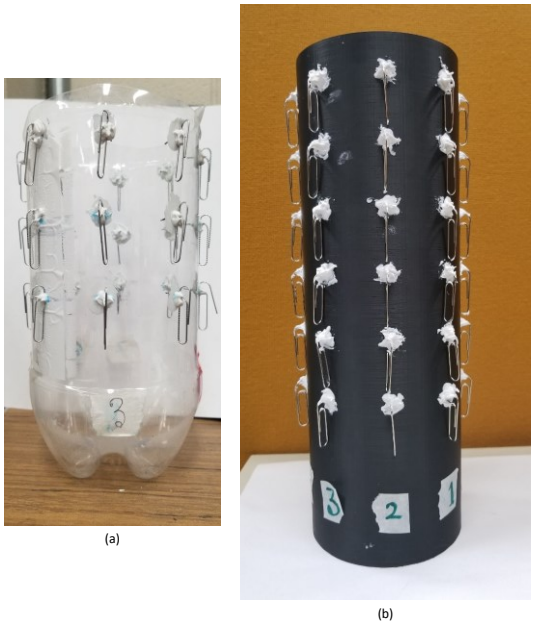

Figure 5.5 Measurement setup containing a) 3 layer of electrodes b) 6 layer of electrodes

5.2.5 EIT reconstruction in EIDORS

Electrical Impedance and Diffuse Optical tomography Reconstruction Software (EIDORS) is an open source publicly available software for image reconstruction of electrical or diffuse optical data. It offers free software algorithms for forward and inverse modeling for Electrical Impedance Tomography (EIT) and Diffusion-based Optical Tomography and allows to share data and promote collaboration between groups working these fields. Such programming encourages innovative work in these fields by giving a reference execution against which new advancements can be looked at and by giving a working programming base, from which new ideas might be manufactured and tested. The sequences of steps in EIDORS for EIT reconstruction is depicted in Figure 5.7 EIDORS software consists of four primary objects such as forward model, data loading, inverse model and inverse solve for image reconstruction. In the Forward problem a known or assumed impedance distribution is used to calculate surface potentials from applied currents using FEM (Finite Element Model). Data collected from the experiment are fed into EIDORS. In the Inverse problem, the measured potentials and applied currents are used to solve for the unknown conductivity/impedance distribution. The EIDORS image basically expresses the reconstructed or simulated conductivity values.

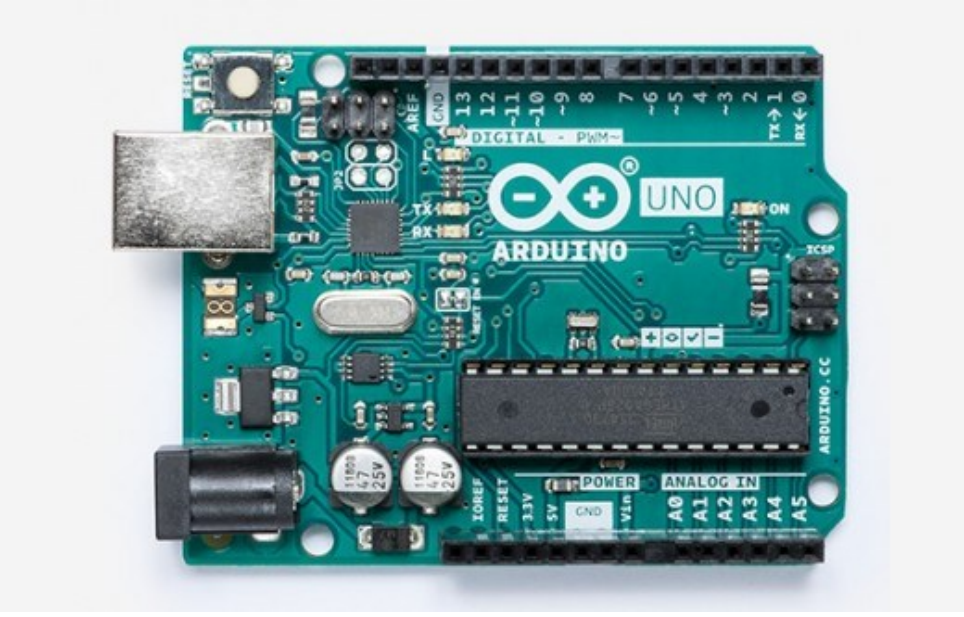

Figure 5.6 Arduino Uno

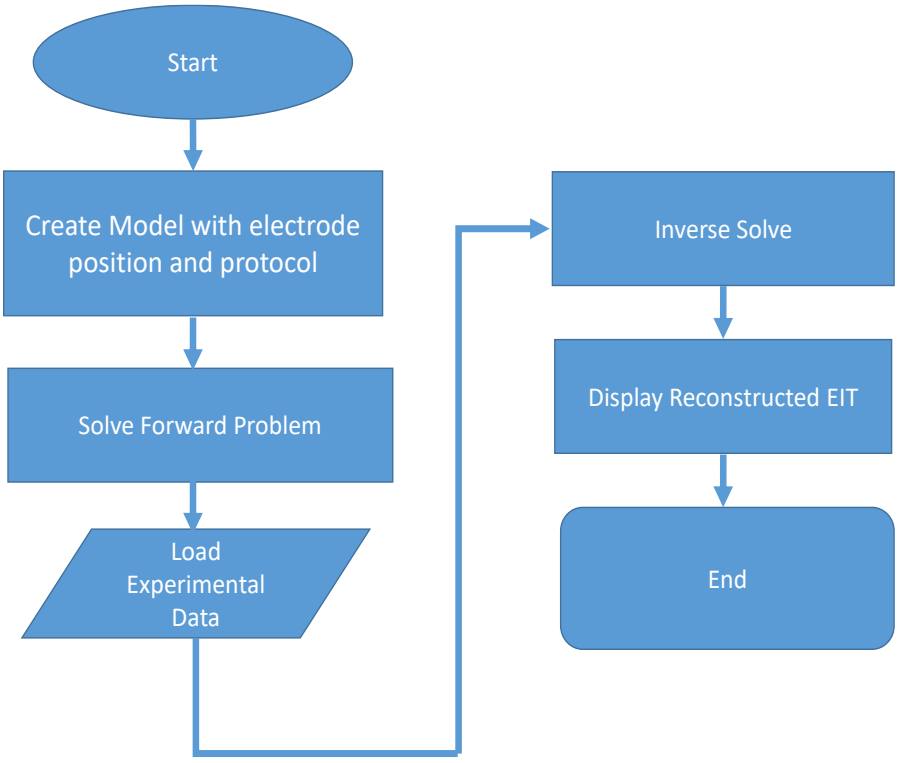

Figure 5.7 Flowchart of EIDORS operation

5.3 Result and Discussion

The reconstruction of EIT is performed using EIDORS in Matlab. In EIDORS, the difference imaging technique is utilized. We feed the impedance distribution for both homogeneous (water) and inhomogeneous (water and object) medium. Exploiting their difference, EIDORS reconstructs the tomographic image of the object placed in the homogeneous medium.

At first, the prototype was tested for 2D EIT imaging and later on, for 3D imaging. For 2D imaging, a cylindrical plastic object was placed at different positions in a cylindrical cup and the corresponding impedance distributions were recorded. After removing the object, the impedance distribution of the homogeneous water medium was captured. Then network mapping was performed to get a sense of the relative position of the object. In the network map, the nodes represent the corresponding positions of the electrodes and the straight lines (i.e. called weights) between the nodes are the inter-electrode impedances. Then the map of homogeneous (water) state was subtracted from inhomogeneous (water and object) state. The difference map offers us some

idea of the position of the object in water medium as observed in Figure 5.8(a, b and c). So this graph mapping verified that the prototype was capturing meaningful data that can locate an object based on their impedance distribution. Next, the reconstruction part of electrical impedance tomography was performed.

For EIT reconstruction, firstly a simulated model was formed which was exactly as same as our experimental setup in term of its shape, electrode positions and the number of electrodes as depicted in Figure 5.8d. At the same time, the model inherited the proper stimulation and measurement protocols same as our experiment. Then both of homogeneous and inhomogeneous data were fed to an inverse solver and 2D EIT reconstruction was performed. Figure 5.8e shows the 2D reconstruction of the object at different positions in water medium. The prototype was also tested for imaging of biological tissue sample (carrot). Different placement of the object and their corresponding tomographic reconstructions are depicted in Figure 5.9.

Next step, the feasibility of utilizing the EIT prototype to detect root in hydroponics and to reconstruct the 3D images was investigated. Placing a weed root in water medium in a cylindrical pot, EIT data were measured using 3 layers of electrodes where every layer contained 8 electrodes. On reconstruction part, inverse solver with differential Gauss-Newton approximation and Tikhonov prior were used. The same electrode was used for both stimulation and measurement, and the injection current value was 1 mA. The hyper-parameter value of the inverse model was chosen as 0.1. The experimental setup, the subject under test (carrot and weed root) and resulting 3D EIT image are depicted in Figure 5.10 and 5.11**.** The reconstructed results allowed us to determine the size, shape, and location of carrot and weed root under test. Thus, the prospect of the system for nondestructive modeling of plant root in hydroponics was also validated.

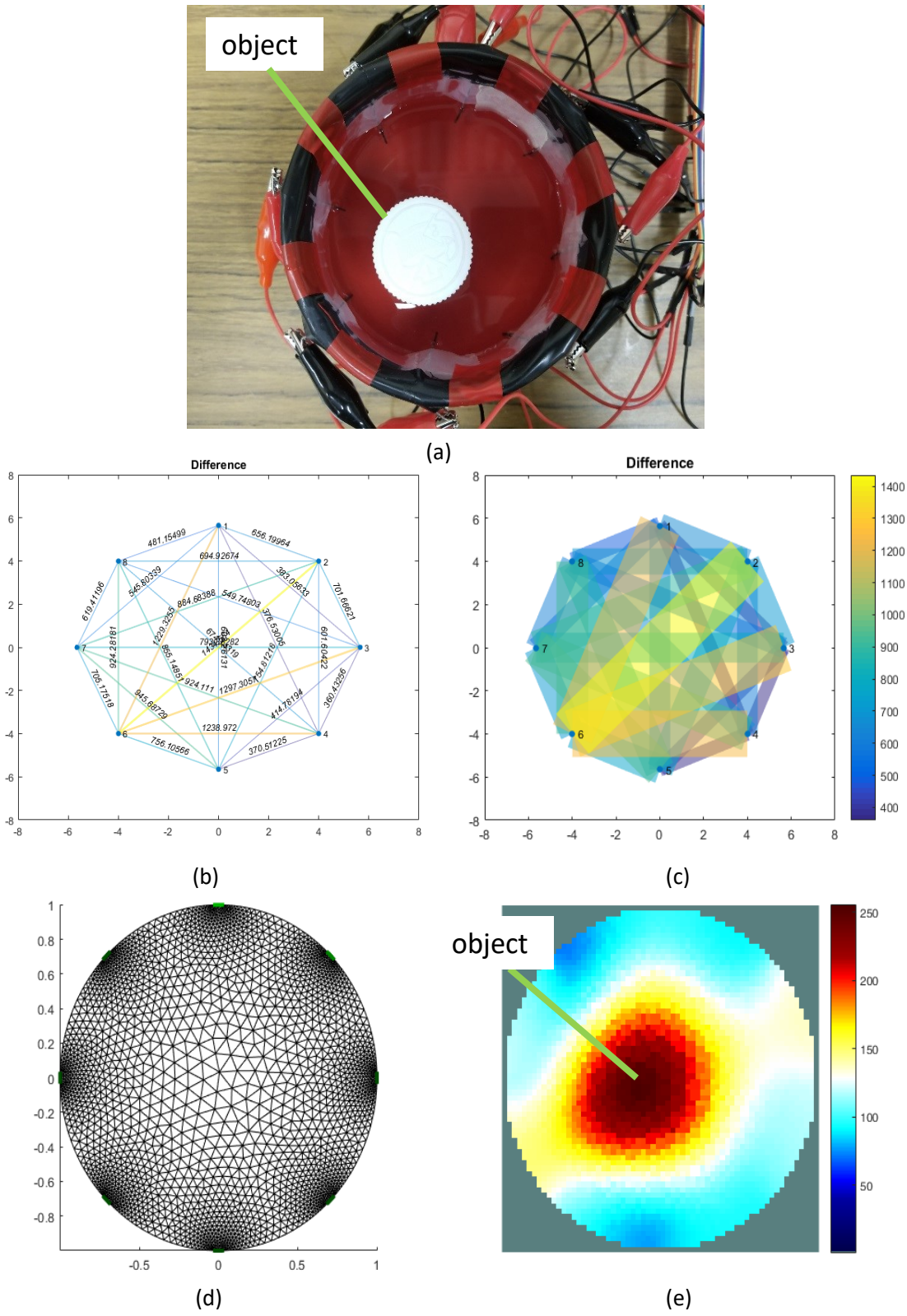

Figure 5.8 a) object in water b) network map of difference impedance c) weighted network map of difference impedance d) 2D FEM mesh e) reconstructed image

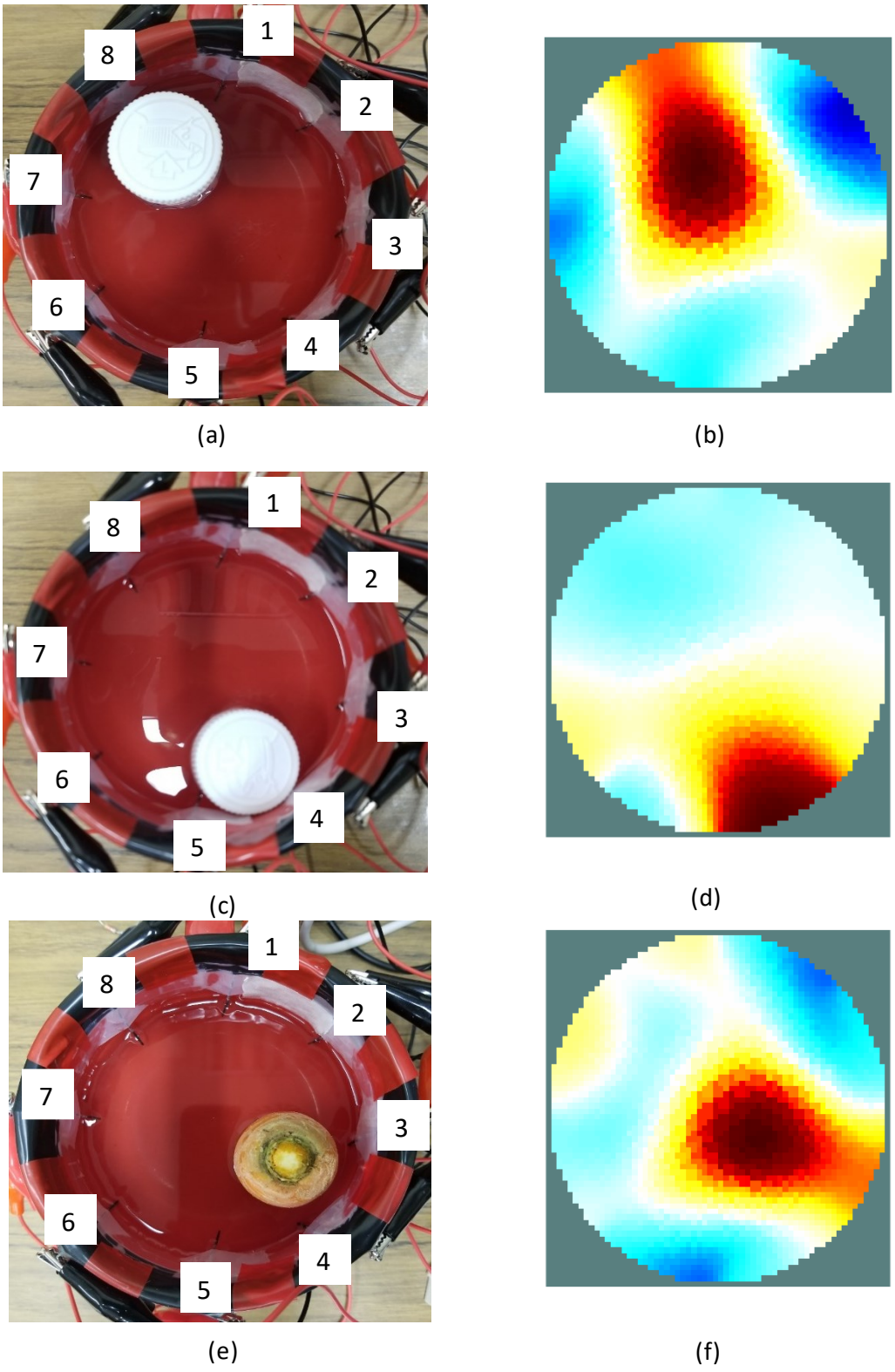

Figure 5.9 Object placement: a) near electrode 8 c) in between electrode 4 and 5 f) close to electrode 3 and 4, and corresponding reconstructed EIT images: b), d) and f).

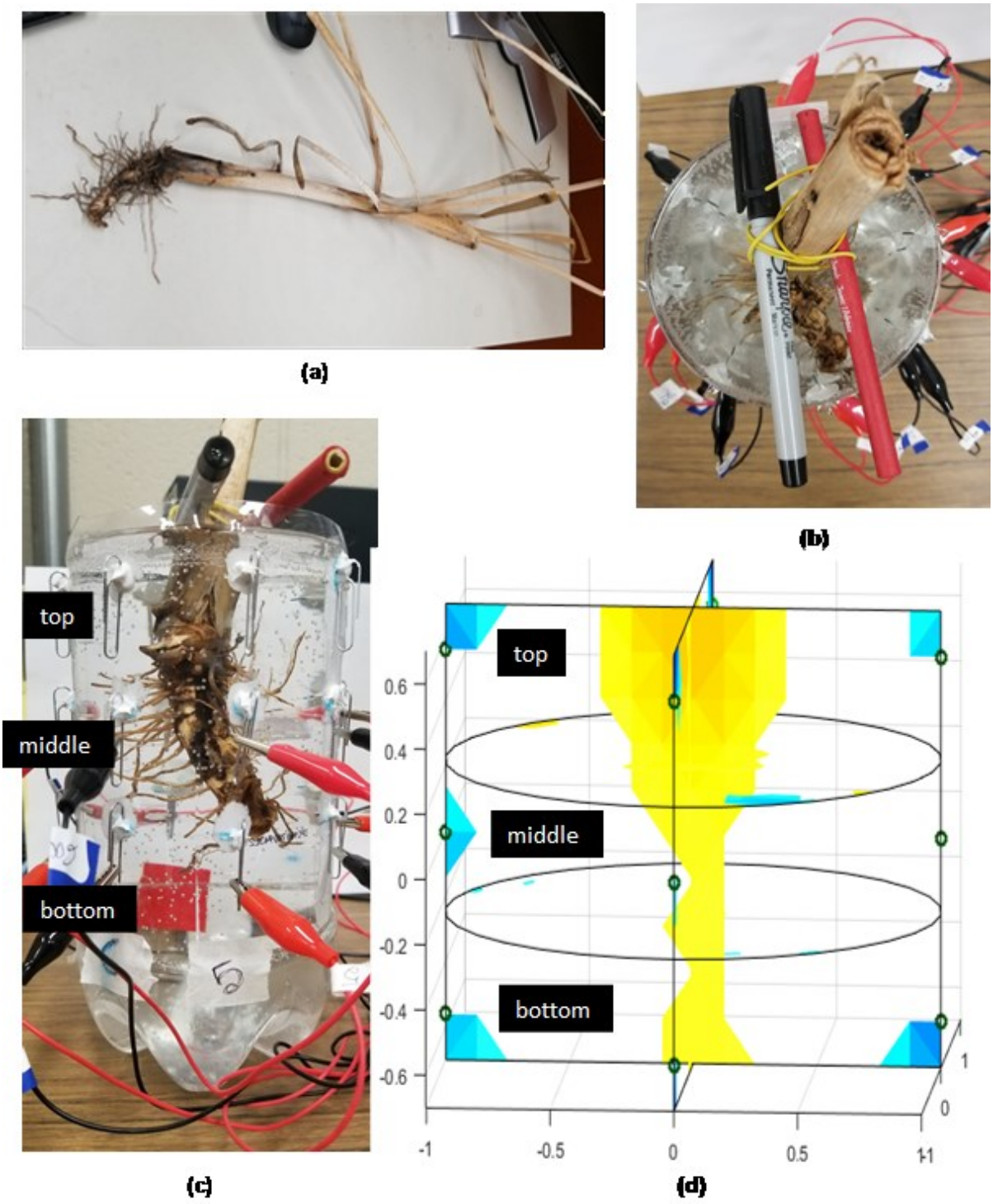

Figure 5.10 a) Weed root b) root in water with top view c) root in water with front view d) reconstructed 3D EIT image.

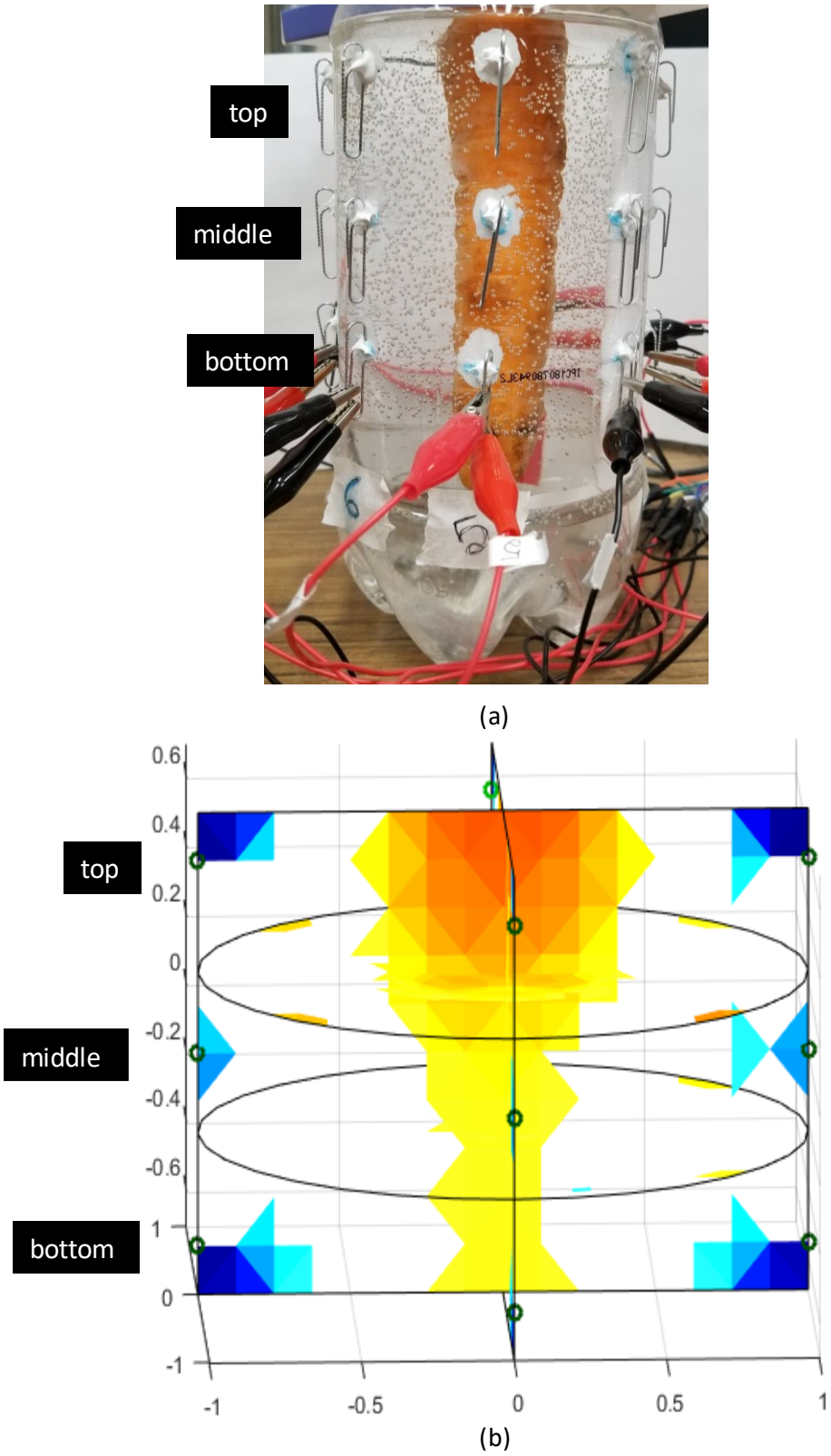

Figure 5.11 a) Carrot in water (front view) b) Reconstructed EIT

5.3.1 Ridge Regression for Biomass Assessment

In regression model, if $\hat{y}$ is the predicted value, then $\hat{y}(\omega, x) = \omega_0 + \omega_1 x_1 + \omega_2 x_2 + ... + \omega_p x_p$ where, ω_0 is intercept and $\omega = (\omega_1, \omega_2 ..., \omega_p)$ are coefficients. Ridge regression addresses some of the problems of Ordinary Least Squares by imposing a penalty on the size of coefficients. The ridge coefficients minimize a penalized residual sum of squares, $\min_{\omega} \| X\omega - y \|_2^2 + \alpha \| \omega \|_2^2$. Here, α >=0 is a complexity parameter that controls the amount of shrinkage: the larger the value of α , the greater the amount of shrinkage and thus the coefficients become more robust to collinearity.

In this work, an investigation was made to assess the biomass of carrot root based on their impedance distribution captured from the EIT device. EIT measurement was performed on 3 carrot samples of different weights which were collected from a local supermarket. After drying those samples for 2 weeks in room temperature (roughly around 20°C) with a relative humidity of 40%, the samples were weighted and those weights were denoted as their corresponding biomass. Experimental carrot samples and their EIT reconstructions are depicted in figure 5.12 .Based on the experimental raw EIT data, a simple mathematical model was formed that can predict the biomass of carrot when corresponding EIT data is fed as input to the model. Proposed Ridge Regression model for biomass prediction is described in equation (5.1).

$$\hat{y}(\omega, x) = \omega_0 + \omega_1 x_1 + \omega_2 x_2 + ... + \omega_6 x_6 \tag{5.1}$$

$$\text{subject to } \min_{\omega} \| X\omega - y \|_2^2 + 0.5 \| \omega \|_2^2$$

where, $\hat{y}$ = predicted biomass,

x_1 = median of impedance distribution of the top electrode layer,

x_2 =standard deviation of impedance distribution of the top electrode layer,

x_3 = median of impedance distribution of the middle electrode layer,

x_4 =standard deviation of impedance distribution of the middle electrode layer,

x_5 = median of impedance distribution of the bottom electrode layer, and

x_6 =standard deviation of impedance distribution of the bottom electrode layer

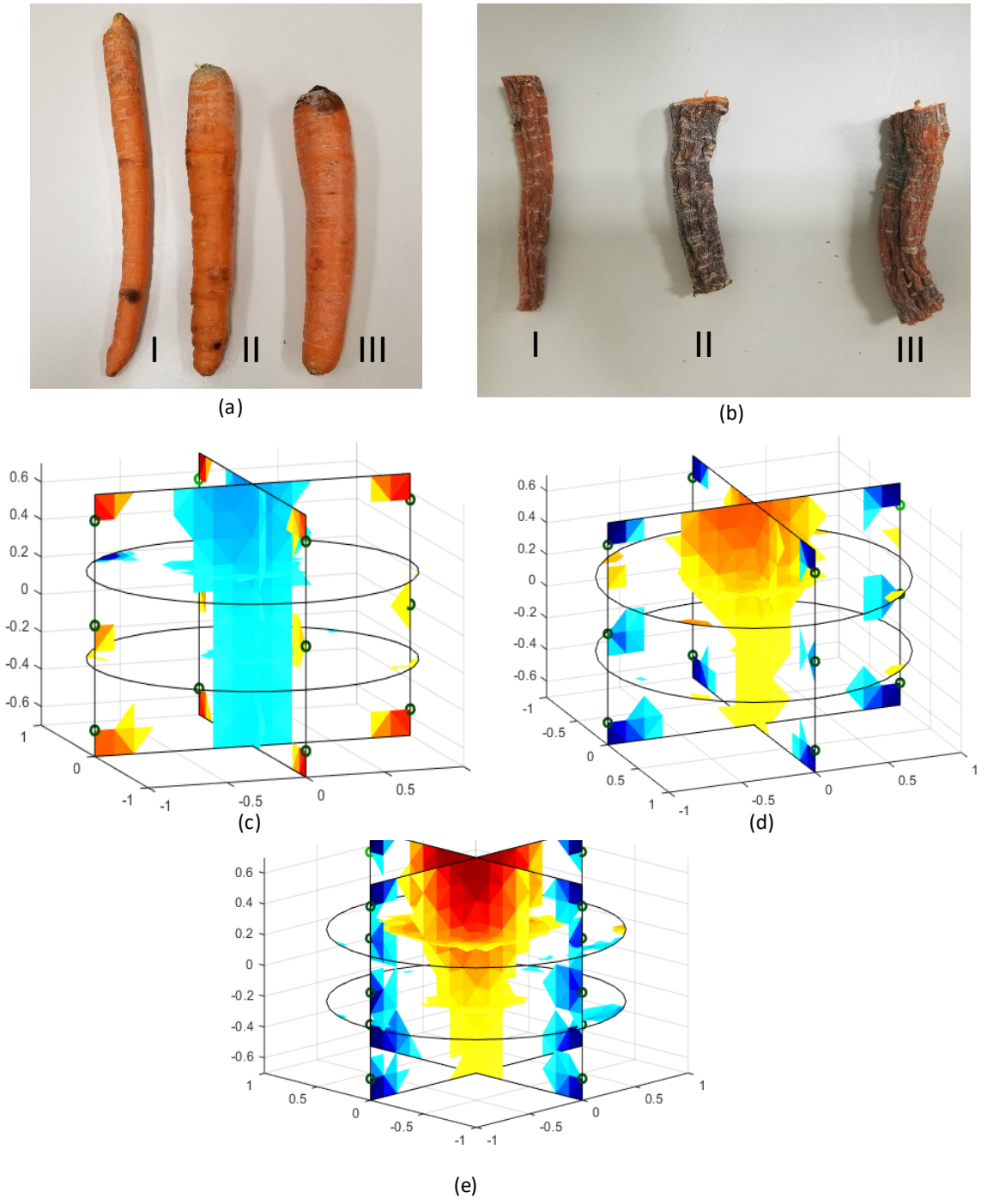

Figure 5.12 Biomass measurement from EIT: a) experimental carrot samples, b) dried carrot cut of the experimental region c) EIT reconstruction of a I, d) EIT reconstruction of a II and e) EIT reconstruction of a III.

After fitting this model with the experimental data, derived intercept and coefficients are described in Table 5.1. Actual biomass and predicted biomass from our Ridge Regression model are presented in Table 5.2

Table 5.1 Intercept and coefficients of the proposed biomass prediction model

ω_0	ω_1	ω_2	ω_3	ω_4	ω_5	ω_6
9.084	0.0882	0.0127	0.1536	-0.0045	0.0325	-0.0097

Table 5.2 Actual and predicted biomass

Actual Biomass in gram	Predicted Biomass in gram	Absolute Error, %
1.89	1.799	5.066
2.7	2.887	6.467
4.19	4.094	2.336

A study on structural and functional imaging of crop root by EIT was conducted by Weigand and Kemna [21]. They were able to image oilseed root in 2D using water-filled rhizotron container with an array of 38 electrodes, whereas, the system in this study is capable of imaging root in 3D and it is really low cost as well. Moreover, this system offers the nondestructive estimation of root biomass with a low percentage of error.

5.4 Conclusion

The work presents the development of a low-cost, low-power, semi-automated, lightweight and small form factor electrical impedance tomography data acquisition system. The system is capable of performing both single and multi-frequency EIT in both 2D and 3D domain. It also offers the ability of imaging living and nonliving subject under test. The reconstructed results allowed us to determine the size, shape, and location of the subject under test. The prospect of the system for nondestructive modeling of plant root in hydroponics was also explored. It was able to image a weed root in 3D in the water medium. Using only readily-available commercial off-the-shelf components, this custom all-in-one system has an approximated module cost of only 120 CAD per unit. The combined performance and cost of this system validates its potential as an effective and low-cost solution for a variety of new and existing applications.

References

[1] R. H. Bayford, "Bioimpedance tomography (electrical impedance tomography)," *Annu. Rev. Biomed. Eng.,* vol. 8, pp. 63-91, 2006.

[2] M. Cheney, D. Isaacson, and J. C. Newell, "Electrical impedance tomography," *SIAM review,* vol. 41, pp. 85-101, 1999.

[3] J. G. Webster, *Electrical impedance tomography*: Taylor & Francis Group, 1990.

[4] T. K. Bera, S. K. Biswas, K. Rajan, and J. Nagaraju, "Improving image quality in electrical impedance tomography (EIT) using projection error propagation-based regularization (PEPR) technique: a simulation study," *Journal of Electrical Bioimpedance,* vol. 2, pp. 2-12, 2011.

[5] T. I. Oh, H. Wi, D. Y. Kim, P. J. Yoo, and E. J. Woo, "A fully parallel multi-frequency EIT system with flexible electrode configuration: KHU Mark2," *Physiological measurement,* vol. 32, p. 835, 2011.

[6] P. Riu, J. Rosell, A. Lozano, and R. Pallà-Areny, "Multi-frequency static imaging in electrical impedance tomography: Part 1 instrumentation requirements," *Medical and Biological Engineering and Computing,* vol. 33, pp. 784-792, 1995.

[7] W. R. Lionheart, "EIT reconstruction algorithms: pitfalls, challenges and recent developments," *Physiological measurement,* vol. 25, p. 125, 2004.

[8] C. W. L. Denyer, "Electronics for real-time and three-dimensional electrical impedance tomographs," Oxford Brookes University, 1996.

[9] D. Holder, A. Rao, and Y. Hanquan, "Imaging of physiologically evoked responses by electrical impedance tomography with cortical electrodes in the anaesthetized rabbit," *Physiological measurement,* vol. 17, p. A179, 1996.

[10] N. Harris, A. Suggett, D. Barber, and B. Brown, "Applications of applied potential tomography (APT) in respiratory medicine," *Clinical Physics and Physiological Measurement,* vol. 8, p. 155, 1987.

[11] T. Meier, H. Luepschen, J. Karsten, T. Leibecke, M. Großherr, H. Gehring*, et al.*, "Assessment of regional lung recruitment and derecruitment during a PEEP trial based on electrical impedance tomography," *Intensive care medicine,* vol. 34, pp. 543-550, 2008.

[12] T. Pham, M. Yuill, C. Dakin, and A. Schibler, "Regional ventilation distribution in the first 6 months of life," *European Respiratory Journal,* vol. 37, pp. 919-924, 2011.

[13] N. M. Zain and K. K. Chelliah, "Breast imaging using electrical impedance tomography: correlation of quantitative assessment with visual interpretation," *Asian Pacific Journal of Cancer Prevention,* vol. 15, pp. 1327-1331, 2014.

[14] M. Kruger, "Tomography as a metrology technique for semiconductor manufacturing," 2003.

[15] T.-C. Hou, K. J. Loh, and J. P. Lynch, "Electrical impedance tomography of carbon nanotube composite materials," in *Sensors and Smart Structures Technologies for Civil, Mechanical, and Aerospace Systems 2007*, p. 652926, 2007.

[16] T.-C. Hou, K. J. Loh, and J. P. Lynch, "Spatial conductivity mapping of carbon nanotube composite thin films by electrical impedance tomography for sensing applications," *Nanotechnology,* vol. 18, p. 315501, 2007.

[17] J. Jordana, M. Gasulla, and R. Pallàs-Areny, "Electrical resistance tomography to detect leaks from buried pipes," *Measurement Science and Technology,* vol. 12, p. 1061, 2001.

[18] J. Hola, Z. Matkowski, K. Schabowicz, J. Sikora, and S. Wójtowicz, "New method of investigation of rising damp in brick walls by means of impedance tomography," in *17th World Conference on Nondestructive Testing*, pp. 25-28, 2008.

[19] P. Linderholm, L. Marescot, M. H. Loke, and P. Renaud, "Cell culture imaging using microimpedance tomography," *IEEE Transactions on Biomedical Engineering,* vol. 55, pp. 138-146, 2008.

[20] T. Sun, S. Tsuda, K.-P. Zauner, and H. Morgan, "On-chip electrical impedance tomography for imaging biological cells," *Biosensors and Bioelectronics,* vol. 25, pp. 1109-1115, 2010.

[21] M. Weigand and A. Kemna, "Multi-frequency electrical impedance tomography as a non-invasive tool to characterize and monitor crop root systems," *Biogeosciences,* vol. 14, pp. 921-939, 2017.

Chapter 6 – Conclusion and Future Work

6.1 Summary

The thesis offers nondestructive characterization of plant by electrical sensing technology. It presents an overview of the theory of Bio-Impedance, electrical impedance spectroscopy (EIS) and electrical impedance tomography (EIT) in chapter 2. EIS measures the variation of impedance over a frequency spectrum by injecting an alternative current with varied frequency. The applied current is small enough not to cause any harm to the sample under test. Measured impedance spectrum can be expressed with an equivalent electrical circuit, and the equivalent circuit represents an electrical model of the sample under test. This equivalent electrical circuit can be exploited for characterization of that object. In EIT, the electrical response of an object is measured from surface boundary from different projection by altering the measurement and stimulation electrodes. Then analyzing those responses by finite element method and solving inverse problem, an impedance distribution of the experimental domain can be achieved. The resulting impedance distribution represents a tomographic image of the subject under test.

In chapter 3, the physiological status of onion undergoing dehydration was monitored nondestructively by electrical impedance spectroscopy. Electrical impedance parameters are found to be sensitive to the alteration of water content in onion. Moreover, to track the physiological changes nondestructively and noninvasively, an equivalent circuit model was proposed that show good agreement with experimental results. In addition, the prospect of electrical impedance spectroscopy to offer nondestructive alternative for assessing moisture content on onion has been explored. Proposed approach can serve as an easily accessible alternative tool for storage period quality assessment of onion.

In chapter 4, the feasibility of electrical impedance spectroscopy to assess the ripening degree of avocado has been explored. A low cost, easily accessible and nondestructive system based on AD5933 impedance analyzer has been investigated in this work. The electrical impedance parameter especially impedance absolute magnitude is found to be most sensitive to ripening progression on avocado. In addition, principal component analysis over frequency dependent electrical response corroborates the hypothesis of distinguishing ripening states based

on EIS. Our classifier based on multiclass Support Vector machines shows excellent discriminant capabilities of EIS technique to track and analyze 4 ripening stages (firm, breaking, ripe and overripe) of avocado. This approach can be a potential alternative to conventional chemical analysis techniques with offering of better time and cost saving and less processing complexity.

Chapter 5 outlines the design and development of a low-cost, low-power, semi-automated, lightweight and small form factor electrical impedance tomography data acquisition system and its application on root imaging. The system is capable of performing both single and multi-frequency EIT in both 2D and 3D. It also offers the ability of imaging living and nonliving subject under test. The reconstructed results allowed to determine the size, shape, and location of the subject under test. The prospect of the system for nondestructive modeling of plant root in hydroponics was also explored. It was able to image a weed root in 3D in water medium. Moreover, the feasibility of assessing biomass nondestructively using raw EIT data was explored. Using only readily-available commercial off-the-shelf components, this custom all-in-one system has an approximated module cost of only 120 CAD per unit. The combined performance and cost of this system validates its potential as an effective and low-cost solution for a variety of new and existing applications.

6.2 Conclusion

This thesis outlines a study on the application of electrical sensing technology, electrical impedance spectroscopy (EIS) and tomography (EIT), for better understanding and characterization of a number of physiological and structural aspects of plant. The thesis has investigated the dehydration process on onion and ripening process on avocado by EIS and performed 3D structural imaging of root by EIT. Equivalent circuit of EIS can simulate the natural drying process of an onion. The proposed mathematical model can serve as an alternating tool to assess moisture content on onion nondestructively. Moreover, EIS technique exhibits the capability of predicting the ripening degree of avocado fruit when a classifier is trained with proper EIS response. The 3D imaging of tap-root in hydroponics can be performed with multiple electrode layer in EIT data acquisition system. Moreover, the dry biomass of root can be predicted with a fairly good accuracy using the raw EIT data. Thus electrical sensing technologies offer the ability to study quantitatively and qualitatively on plant physiology, and provide a promising step towards food security and agricultural sustainability.

6.3 Future work

Electrical sensing technologies, EIS and EIT, have shown their feasibility in exploring plant physiological and structural traits such as natural dehydration, moisture content, ripening degree and root structure. However, there are still lot of research opportunities on these fields. Some of the crucial broad level future research direction includes –

- During unrefrigerated storage of onion, EIS was used to analyze dehydration process and to assess moisture content nondestructively and noninvasively. This technique can be extended for other perishable vegetables for storage period quality assessment. Future works may also include the development of an automated moisture content monitoring system for vegetables based on EIS by combining environment controller, wireless communication module and portable monitoring device.
- The ripening degree of avocado was determined using EIS and machine learning technique. Proposed system can be extended and tested to other fruits for analyzing their ripening dynamics nondestructively by EIS. It should be addressed in future studies and a database on fruit ripening can be established containing a large number of groups and samples and their corresponding EIS parameters.
- The quality factors (ex. moisture content, ripening degree) of fruit and vegetables during ripening and storage will be affected by temperature and humidity [1] . All the experiments in this investigation were performed at room temperature. It is suggested that further studies may include observation of fruits and vegetables quality with different temperature and humidity variations.
- Proposed EIT system shows its merit in structural imaging of root. More studies need to be conducted on EIT for investigation and determination of root's other physiological, functional and structural characteristics like root length and density, water stress, nutrient intake, etc.
- The designed EIT system is fully automated for 2D imaging but it is semi-automated for 3D domain. By increasing the number of multiplexer switching units, it can be made fully automated for 3D imaging as well. Moreover, better resolution on reconstruction part can be achieved by increasing the number of electrodes per layer [2].

- The designed EIT system exhibits its capability of imaging the tap root in hydroponics. Future efforts and studies are needed to offer imaging of fine roots. In low frequency, electric polarization in root occurs due to the charge migration from root surface to electrolytes. But at higher frequency, the polarization occurs due to root's actual structure [3]. Since the impedance converter board in this study operates in KHz range, the MHz or GHz range responses were unexplored. Replacing the current impedance analyzer by a high frequency one, the feasibility of imaging fine roots can be explored in future endeavors.

References

[1] R. Paull, "Effect of temperature and relative humidity on fresh commodity quality," *Postharvest biology and technology,* vol. 15, pp. 263-277, 1999.

[2] V. Chitturi and F. Nagi, "Spatial resolution in electrical impedance tomography: A topical review," *Journal of Electrical Bioimpedance,* vol. 8, pp. 66-78, 2017.

[3] M. Weigand and A. Kemna, "Multi-frequency electrical impedance tomography as a non-invasive tool to characterize and monitor crop root systems," *Biogeosciences,* vol. 14, pp. 921-939, 2017.